Use of the Traceable Kinase Method to Identify Protein Substrates that Mediate PKCα-Stimulated Motility in Human Breast Cells

By

Thushara Preeni Abeyweera

A dissertation submitted to the Graduate Faculty in Biochemistry in partial fulfillment of the requirements for the degree of Doctor of Philosophy, The City University of New York.

2007

UMI Number: 3295017

UMI Microform 3295017

Copyright 2008 by ProQuest Information and Learning Company.
All rights reserved. This microform edition is protected against
unauthorized copying under Title 17, United States Code.

ProQuest Information and Learning Company
300 North Zeeb Road
P.O. Box 1346
Ann Arbor, MI 48106-1346

This manuscript has been read and accepted for the Graduate Faculty in Biochemistry in satisfaction of the dissertation requirement for the degree of Doctor of Philosophy.

Dr. Susan A. Rotenberg

Date

Chair of Examining Committee

Dr. Lesley Davenport

Date

Executive Officer

Dr. David Foster

Dr. Adriana Haimovitz-Friedman

Dr. Karl Fath

Dr. Joni Seeling
Supervisory Committee

THE CITY UNIVERSITY OF NEW YORK

ABSTRACT

Use of the Traceable Kinase Method to Identify Protein Substrates that Mediate PKCα Stimulated Motility in Human Breast Cells

By

Thushara Preeni Abeyweera

Advisor: Dr. Susan A. Rotenberg

Identification of the proteins that are phosphorylated by PKCα posed a major challenge until the introduction of the Traceable Kinase Method. This approach consists of engineering the ATP binding site of PKCα so that it can accommodate a larger analogue of ATP, such as N^6-phenyl-ATP, that cannot be bound by the wildtype PKCα or presumably any other protein kinase. [γ-^{32}P]-N^6-phenyl-ATP was used by the mutant PKCα to radiolabel substrate proteins that co-immunoprecipitated with mutant PKCα from a total human breast cell lysate. Following resolution of radiolabeled proteins by SDS-PAGE and autoradiography, mass spectrometry identified α6-tubulin one of several PKCα substrates. Four potential PKC consensus sites of phosphorylation of α6-tubulin were identified and mutated to Asp (D) in order to simulate phosphorylation. Motility assays with cells transfected with each mutant identified Ser-165 as the only site in α6-tubulin mutants whose pseudo-phosphorylation reproduced the level of motility previously ascribed to PKCα. The S165D-α6-tubulin was not incorporated into microtubules. Taken together, the results support a model in which phosphorylation of α6-tubulin at Ser-165 by PKCα leads to cell movement by preventing incorporation of α6-tubulin into microtubules.

ACKNOWLEDGEMENTS

I would like to thank my mentor, Dr. Susan A. Rotenberg. I could not have imagined having a better advisor and mentor for my PhD, and without her help and guidance I would never have finished. Thank you to my examiners, Dr. David Foster, Dr. Karl Fath, Dr. Adriana Haimovitz-Friedman, and Dr. Joni Seeling for managing to read the whole thesis so thoroughly, and for good discussions. I would also like to thank all the rest of the academic and support staff of the Department of chemistry and Biochemistry at the Queens College of the City University of New York.

My special thanks to Dr Areti Tsiola for assistance in operating the confocal microscope, Dr. Corinne Michels, and Dr. Saima Cheema for their expert advice.

Dr. Rotenberg's group members are thanked for numerous stimulating discussions and help with experimental setup. In particular, I would like to acknowledge the help of Dr. Regina M. Sullivan and Mr. Xiang Yu Chen for their support.

I am grateful to Dr. Sunil Dehipawala and Shantha Amarasinghe for being my best friends, for their moral support, and to thank them for their care and attention.

Finally, I am forever indebted to my parents for their understanding, endless patience and encouragement when it was most required. I am also grateful to my husband and my daughter, Nishmi for their support and understanding.

Dedication

This thesis is dedicated to my parents and all my past and present teachers.

TABLE OF CONTENTS

List of Tables **Page**

List of Figures **Page**

Abbreviations Used:

ADP	adenosine diphosphate
ATP	adenosine triposphate
A*TP	N^6-phenyl-ATP
BSA	bovine serum albumin
CDK2	cyclin-dependent kinase 2
DAG	diacylglycerol
EDTA	N, N, N', N'-ethylenediaminetetraacetic acid
EGTA	ethylene glycol-bis (2-aminoethylether) - N, N, N', N'-tetraacetic acid
FBS	fetal bovine serum
GFP	green fluorescent protein
hnRNP	heterogeneous ribonucleo-protein
JNK	c-Jun amino terminal kinase
KESTREL	Kinase Substrate Tracking and Elucidation
MAPK	mitogen-activated protein kinase
MARCKS	myristoylated alanine-rich C kinase substrate
MBP	myelin basic protein
NDPK	nucleoside diphosphate kinase
PCR	polymerase chain reaction
PDK-1	Phosphoinositide-dependent kinase-1
PICK	Protein that Interacts with C-Kinase
PKA	cAMP-dependent protein kinase
PKC	protein kinase C

PS	phosphatidylserine
RACK	Receptor for Activated C Kinase
STICKs	Substrates That Interact with C Kinase
TPA	12-O-tetradecanoylphorbol-12,13-acetate

CHAPTER 1

INTRODUCTION

Protein kinase C (PKC) is a Ca^{2+}- and phospholipid-dependent protein kinase that phosphorylates serine and threonine residues in many target proteins. This multifunctional enzyme was first identified in bovine cerebellum by Nishizuka and co-workers.[1] It was subsequently found that PKC exists as a family of isoforms that exhibit different sub-cellular locations and modes of regulation by intracellular stimuli. Once activated, PKC isoforms act as upstream components of various signaling pathways that govern mitogenesis and proliferation of cells, apoptosis, platelet activation, remodeling of the actin cytoskeleton, and cell movement.

Malfunctions in PKC-signaling pathways have been implicated in the development of multiple human diseases, such as diabetes, Alzheimer's disease, cardiovascular disorders, and central nervous system dysfunctions. However, by far the most prominent association of PKC with disease has been in the promotion and progression of cancer[2]. The discovery that PKC is the primary receptor for 12-*O*-tetradecanoylphorbol-13-acetate (TPA), a potent tumor promoter, provided a direct link between PKC and carcinogenesis. Studies with cell models have since shown that each cell type has a characteristic isoform expression profile and that individual PKC isoforms have distinct or overlapping roles in generating the transformed phenotype.[3] Until recently, elucidation of the substrates and the pathways of specific PKC isoforms represented an insurmountable challenge.

Due to the role of PKC in many cancers, a few inhibitors that have selectivity for certain isoforms have been developed. These inhibitors have anti-cancer properties in cells and animal models, but their clinical efficiency is low. One possibility of increasing the efficiency of such drugs would be to design a cocktail drug that targets PKC and its immediate substrates. Therefore, identification of PKC direct substrates could provide an avenue for improving strategies of chemotherapy.

Enzymatic Mechanism of Protein Kinases

In addition to a protein substrate, all ser/thr-protein kinases bind ATP at their active sites. Once bound, the γ-phosphate of ATP is transferred by an "in-line" mechanism to a Ser or Thr residue of the protein substrate. After phosphorylation, the product is released from the kinase. The order of steps may differ for different kinases. For example, some kinases bind their protein substrates before binding ATP and others release ADP before releasing the protein substrate. The rate-limiting step can also vary between different kinases[4]. Protein kinases share a common secondary structure of roughly 250 residues known as the "kinase fold" or "kinase core". This core is composed of a set of highly conserved residues that are directly involved in the formation of the active site and includes the nucleotide-binding pocket and the site of phosphoryl transfer. ATP binds in a cleft in the kinase core so that the adenosine moiety is buried in a hydrophobic pocket with the phosphate backbone orientated outwardly towards the external medium. The protein substrate binds along the cleft and a set of conserved residues within the catalytic domain mediate the transfer of the terminal γ-phosphate of ATP to the hydroxyl oxygen of either a Ser (or Thr) residue of the substrate. The mechanism of phosphorylation by the

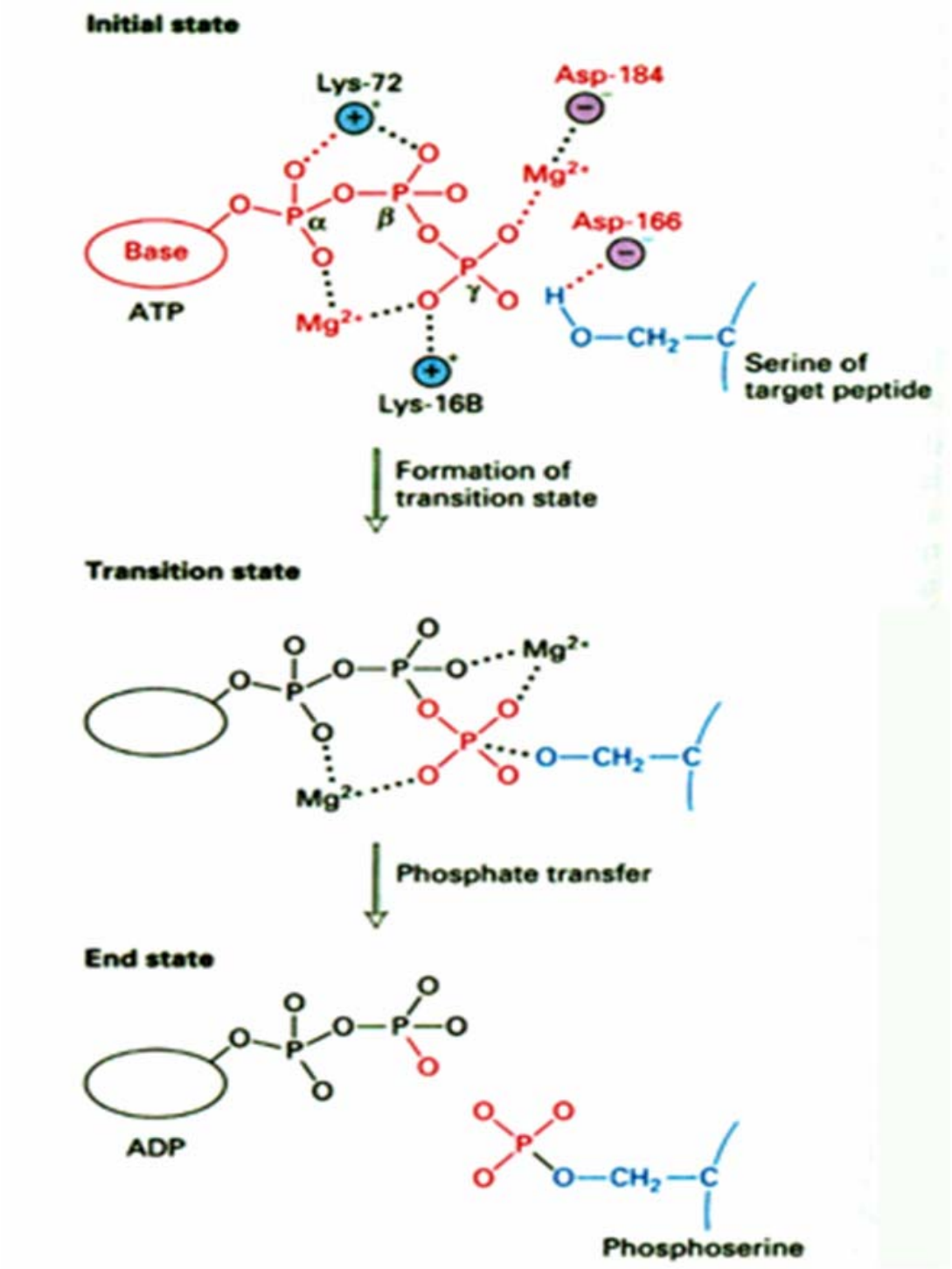

Figure 1. **Catalytic mechanism of a protein kinase**. The in-line phosphoryl transfer carried out by a protein kinase, as shown for the cAMP-dependent protein kinase (PKA). [Taken from: http://fig.cox.miami.edu/~cmallery/255/255enz/mcb3.18.mechanism.jpg]

cAMP-dependent protein kinase (PKA) is shown in Figure 1. A lysine residue (Lys-168) and Mg^{2+} enable phosphoryl transfer by delocalizing electrons of the phosphate group. Asp-166 abstracts a proton from the hydroxyl group of the serine in the bound target peptide, whereupon the oxygen of the serine side chain binds to the γ-phosphate to form a pentavalent transition-state intermediate. The phosphoester bond between the β and γ phosphates is broken to form a phosphorylated serine side chain and ADP.

The catalytic domain of PKC has approximately 40% amino acid identity with PKA, and the ATP binding site of all PKC isoforms is identical. Of those residues that are important in PKC catalysis, the ATP-binding lysine residue (Lys-368) is shown in the crystal structure of PKCθ (Figure 2).

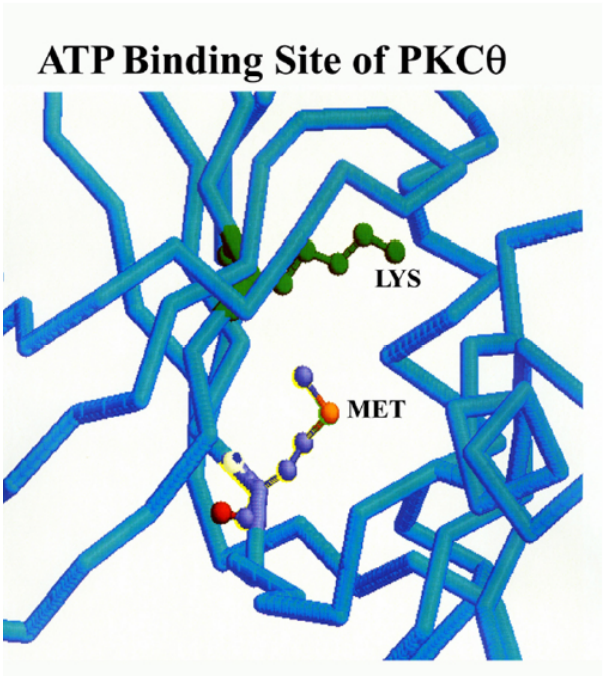

Figure 2. **ATP-Binding Site of PKCθ.** The ATP-binding lysine in PKCα is located at Lys-368 (green sidechain). Also highlighted is a Met sidechain that corresponds to Met-417 in PKCα.

Family Members, Structure, and Activation

PKC activity is expressed by a family of structurally-related isoforms. At present, eleven mammalian isoforms have been identified. The PKC family can be broadly divided into three groups that differ in their sequence and cofactor requirements. These are:

- Conventional (c) PKC isoforms (α, β_1, β_{11}, and γ) – require Ca^{2+} and diacylglycerol (DAG) to become activated.
- Novel (n) PKC isoforms (δ, ε, η, θ, and μ) - require only DAG to become activated.
- Atypical (a) PKC isoforms (ζ and ι) - require neither Ca^{2+} nor DAG.

All PKC isozymes consist of a single polypeptide chain that contains an amino-terminal regulatory domain and a carboxy-terminal catalytic domain linked by a hinge region. Figure 4 shows a schematic of the structural domains of the three subclasses of PKC isozymes. The catalytic domain is very similar in all PKC isoforms but the regulatory domains have variable regions that define their respective responses to activating cofactors[5,6,7]

Activation of PKC results in its translocation from the cytoplasm to the plasma membrane where it binds and phosphorylates its substrates (Figure 3). Several events occur to enable activation. The regulatory domain in the amino terminal portion of PKC contains an auto-inhibitory pseudosubstrate domain, and one or two membrane-targeting motifs, namely the C1 and C2 domains. In the inactive enzyme, the pseudosubstrate segment is tucked into the substrate binding domain thereby preventing the binding of

protein substrates. The C1 region is present in all PKC isoforms and consists of two tandem zinc-finger motifs. This domain binds its physiological activator diacylglycerol (DAG) or TPA (a tumor promoter found in plants that is a functional analogue of DAG) in all but the atypical PKCs. cPKCs and nPKCs have two C1 domains that serve as a membrane-targeting module. Once bound to PKC, DAG provides the means to bind the

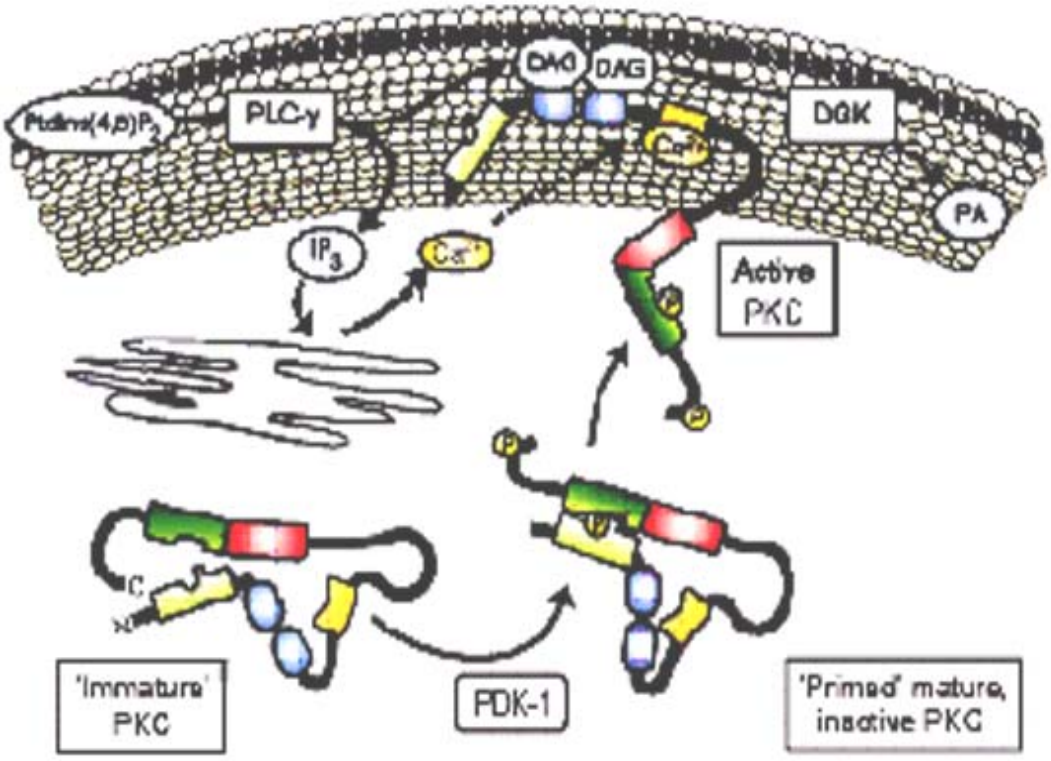

Figure 3. **Activation of classical and novel PKC isoforms**[8] The first step to PKC maturation involves phosphoinositide-dependent kinase (PDK-1)-dependent phosphorylation of a conserved threonine (T) residue in the activation loop, followed by auto-phosphorylation of conserved S or T both at the turn motif and at the hydrophobic motif. The hydrophobic motif is the docking site of PDK-1.

C1 region to the membrane. The C2 region, which houses the Ca^{2+} binding site, is present in cPKCs and nPKCs and accounts for their sensitivity to Ca^{2+}. In cPKCs, this 12-kDa domain serves as a second membrane–targeting module that binds anionic phospholipids

such as phosphatidylserine (PS), in a Ca^{2+}-dependent manner[5]. Generation of DAG and Ca^{2+} as second messengers induces conformational changes in PKC such that the pseudosubstrate is released from the active site and the C1 and C2 domains engage the membrane. Thus, C1 and C2 domains function as independent membrane-targeting modules and can independently recruit PKC to membranes. A hallmark of PKC activation in cells is its translocation to the plasma membrane.

Before PKC is competent to undergo activation by DAG and Ca^{2+}, it must first be phosphorylated at three conserved positions in the kinase core. Phosphoinositide-dependent kinase-1 (PDK-1) phosphorylates PKC at a Thr residue in the activation loop that in turn triggers autophosphorylation of two carboxyl-terminal sites: the turn motif and the hydrophobic motif[9]. Figure 4 shows the three sites of phosphorylation. These positions are not only conserved among all PKC isoforms, but also among other AGC family members.

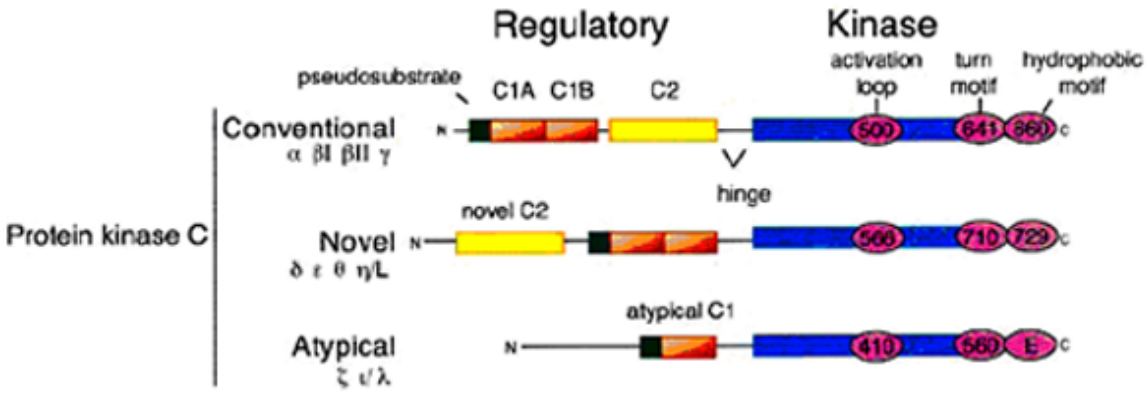

Figure 4. Schematic of primary structures of PKC family members[5]

The biological function of PKC depends on its correct spatial distribution within the cell. This localization is mediated by binding partners for PKC[10]. Some binding proteins regulate multiple PKC isoforms, whereas others (such as anchoring proteins) control the sub-cellular distribution of specific isoforms. One such binding partner, called the Receptor for Activated C Kinase (RACK), anchors the active conformation of phosphorylated PKC at specific sub-cellular locations. Whereas another protein group designated as Substrates That Interact with C Kinase (STICKs) bind inactive, phosphorylated PKC[11]. These proteins position PKC near their substrates, near regulators of activity such as phosphatases and kinases, or in a specific intracellular compartment.

Studies of PKCα in Human Breast Cell Lines

PKC is frequently highly expressed in human breast tumors[12]. To study the impact of a single PKC isoform, investigators previously used MCF-7 cells, a non-metastatic human breast cell line. When MCF-7 cells were engineered to over-express PKCα, proliferation increased, tumorigenicity increased, and cells lost their epithelial appearance[13]. However, the over-expression of PKCα in these cells coincided with increases in PKCβ. This result indicated that in MCF-7 cells, the two isoforms are mutually regulating. Further complicating efforts to identify the phenotypes induced by a single isoform was the problem of multiple variants of MCF-7 cells. Thus, different laboratories that addressed the question of PKCα in MCF-7 cells found conflicting results. The problem was mitigated in 1990 when the MCF-10A cell line was introduced. These cells are non-transformed and non-tumorigenic human breast epithelial cells[14]. Western blot analysis showed that these cells have negligible levels of PKCα and thus provide a very low

background for studying the effects that follow engineered expression of PKCα. When MCF-10A cells were stably transfected with PKCα, proliferation decreased, motility and adhesion increased, redox activity decreased and cell morphology was dramatically altered. Importantly, these phenotypes could be attributed to PKCα alone since the expression of other PKC isoforms remained unchanged[15,16].

Tumors often express high levels of PKC that has been linked with cancer metastasis. Metastasis is a multi-step process in which tumor cells lose their contact with neighboring cells, migrate from the primary tumor into the circulation, and invade and colonize other sites to establish secondary tumors[17]. In most cases, tumors that stay confined to one organ will not be fatal, and surgical removal or irradiation of these tumors will often result in complete cure. Tumor cells that have spread to other organs are often difficult to treat. Therefore, a complete understanding of each step involved in metastasis is a key to developing new therapies that suppress the growth and dissemination of metastatic cells. The process of metastasis entails cell adhesion and migration, phenomena that both involve the activity of PKC.

The Cytoskeleton and Cell Movement

Although cell movement was observed as early as 1675 when van Leeuwenhoek saw cells crawl across his microscope slide, the molecular mechanisms behind cell movement have become a scientific focus only in the past few decades[18]. The cytoskeleton provides a molecular framework that makes cell migration possible. This subcellular structure consists of actin filaments, microtubules, and intermediate filaments. These cytoskeletal

elements produce the motor force and critical physical support during cell movement. Unfortunately, the cytoskeletal-based mechanism so central to cancer metastasis remains poorly understood. One of the hurdles in studying the cytoskeleton lies in its complexity as well as in the dynamic nature required for its physiological function.

Motile cells display a characteristic polarization of the actin cytoskeleton. Actin filaments polymerize in the protruding edge of the cell whereas actin filament bundles contract within the cell body, which results in retraction of the trailing edge. The dynamic organization of the actin cytoskeleton provides the force for cell motility and is regulated by small GTPases of the Rho family, in particular Rac1, RhoA and Cdc42[19]. Although the microtubule cytoskeleton is also polarized in a migrating cell, and microtubules are essential for the directed migration of many cell types, their role in cell motility is not well understood at a molecular level. The shape of the microtubule network remodels dynamically in order to regulate cell functions to respond to stimuli from the environment. However, it is still unclear as to what molecular mechanisms modulate such behavior. Therefore identifying molecular mechanisms that regulate the cytoskeleton-dependent processes associated with metastasis progression is key to developing new therapies to treat and prevent metastatic disease.

Microtubules are cytoskeletal elements that are essential for various cellular functions[20]. They consist of polymers of globular tubulin subunits that are organized in a cylindrical tube composed of protomers, the structural unit of microtubules. A protomer consists of heterodimer of α and β tubulin isotypes. Each tubulin monomer binds a GTP, which is

non-exchangeable when it is bound in the α subunit, and exchangeable when bound in the β subunit. Both exist in several isotypes and undergo a variety of posttranslational modifications[21] such as polyglutamylation, polyglycylation, tyrosine phosphorylation, and detyrosination. A number of these modifications are unique to tubulin[22], but the precise functional consequences of these modifications remains unclear.

A number of components are involved in regulating the dynamic structure of the cytoskeleton. It is known that phorbol esters can stimulate cell migration[23] and that it causes an immediate effect on the cytoskeleton[24]. Since phorbol esters are well known activators of classical and novel PKC isoforms, it can therefore be assumed that one or more PKC isoforms are involved in changes to cytoskeletal structure that promotes cell migration. PKCs also localize to discrete cytoskeletal structures, indicating that they are positioned to interact with and phosphorylate cytoskeleton-associated proteins[25]. In support of this observation, a cytoskeletal protein named myristoylated alanine-rich C kinase substrate (MARCKS), which binds actin, undergoes phosphorylation by PKC and consequently dissociates from the cytoskeleton, thus initiating its reorganization.

PKC in Cancer and as a Chemotherapeutic Target

Most cells express several conventional and novel PKC isoforms, all of which can be activated by phorbol esters. Although PKCs are clearly implicated in tumor promotion and cytoskeletal remodeling, the specific roles of the individual isoforms have yet to be determined. One approach to studying the roles of individual PKCs in tumor progression is to identify changes in PKC isoform expression that correlate with progressive stages of

transformation. Functional relevance can then be assessed by increasing or decreasing individual PKC activities by over-expressing wild-type or dominant-negative constructs, respectively[15]. In previous studies, the Rotenberg lab investigated the potential involvement of PKCα over-expression on the proliferation, adhesion, and motility of MCF-10A human breast cells[15]. Their findings indicated that PKCα suppresses proliferation while increasing the motility of these cells.

PKCα continues to be an attractive target for design of anti-cancer agents. Research groups have developed several ways to target this enzyme therapeutically, such as with antibodies or small molecules that either block the kinase-substrate interaction or inhibit the ATP binding site. A number of protein kinase inhibitors have already been developed and approved for cancer treatment. Midostaurin is an example of a PKC inhibitor that can be used for anticancer therapy[26]. In clinical trials however, specific blocking of only one of the kinases involved in these signaling pathways by anti-sense DNA or siRNA has been associated with limited success. Therefore by understanding the complexity of the signaling pathways that support cell movement and metastasis, simultaneous inhibition of the kinase and its immediate substrates could strengthen the anti-cancer effects of chemotherapy.

The Problems of Identifying Direct Substrates of Protein Kinases

The recent sequencing effort of the entire human genome revealed that there are approximately 500 human protein kinases[27]. The three-dimensional structures of several protein kinases have now been determined, and their modes of interaction with substrates

and inhibitors are becoming increasingly understood at the molecular level. Although we have a well-developed understanding of protein kinases, the same cannot be said for their immediate protein substrates which are largely unidentified. This fact is especially true for the PKC family, which is particularly important in cell migration and metastasis. Therefore, an important direction in PKC-related research is to identify physiologically relevant substrates and pathways for individual isoforms and to assess the degree of overlap in their substrate specificity.

Since the discovery of PKC in 1977, many proteins have been identified as substrates in vitro[2]. Some of the known intracellular PKC substrates are MARCKS, Lamin A and C, elongation factor 1, β4 integrin, adducin, pleckstrin[28] and heterogeneous ribonucleo-protein A1 (hnRNP A1)[11,29]. Although some substrates of PKC have been identified, the diverse pathways governed by PKC within the cell suggest that many unknown substrates remain to be identified.

Several techniques have been used in the last 20 years to identify and characterize PKC substrates in cells but they have been hampered by both conceptual and technical limitations. There are a number of factors that complicate identification of substrates of a particular kinase. First, the enormous size of the kinase superfamily and the extent of protein phosphorylation in the cell make it inherently difficult to assign a phosphoprotein to a specific kinase. Secondly, kinases often display little preference for a particular sequence flanking the phosphorylated residue (consensus sequence), so identification of potential substrates from a predicted amino acid sequence is very difficult. It is also well

known that many important kinases are redundant in target specificity. Thus, information from gene knock-out studies and similar methods will provide only a partial view of the many interactions in which kinases participate. For these reasons and others, determining the target proteins of one kinase in a specific signaling cascade has proven to be intractable by conventional methods[30]

Classical methods for identifying protein kinase substrates are based on making an educated guess and then incubating the purified candidate substrate with a purified protein kinase, usually in the presence of $MgCl_2$ and [γ-^{32}P]-ATP. Although this technique has been extremely useful in the past, it cannot be used where there is little or no knowledge of the likely substrate. Novel protein kinase substrates have been also identified through the use of a phage display library of proteins that is immobilized on a nitrocellulose membrane and then phosphorylated by the purified kinase in the presence of [γ-^{32}P]-ATP. Phage that encode substrates of the kinase are detected by autoradiography and the identity of the substrate can then be determined by sequencing the cDNA insert. This quick and relatively simple method has been used successfully to find mitogen-activated protein kinase (MAPK)-interacting kinase, a substrate of ERK1 and the p38 MAPK[31]. Also, cell lysates can be incubated with purified protein kinase in the presence of $MgCl_2$ and [γ-^{32}P]ATP, and the resultant phosphorylated proteins are purified by conventional protein purification techniques. Alternatively, proteins can be sub-fractionated before phosphorylation either by protein kinases that are endogenous to that fraction or by a purified protein kinase that is added to the reaction mixture. This approach, called KESTREL (*k*inas*e* *s*ubstrate *tr*acking and *el*ucidation), reduces problems

owing to high ATPase activity in cell lysates, and decreases the complexity of the sample for consequent substrate identification by mass spectrometry. The technique also uses manganese in place of magnesium in an attempt to reduce background phosphorylation. An obvious limitation of this approach is that it can only be used with protein kinases that bind Mn^{2+}-ATP.

Although these methods are highly informative, they carry some serious drawbacks. First, those methods that exploit semi-purified experimental systems could give false positives since protein kinases are known to show promiscuous activity *in vitro*. In this regard, sub-cellular compartmentation of proteins might prevent a protein substrate from becoming effectively exposed to the kinase, even though that protein might be an excellent substrate *in vitro*. Second, proteins expressed in prokaryotic systems may not fold appropriately or carry the necessary post-translational modifications (*e.g.* phosphorylation events that prime the enzyme may be absent). Last, identification of direct substrates of kinases is difficult due to the overlap of a consensus phosphorylation sequence among related kinases: a protein that is phosphorylated at a specific site could have been produced by more that one kinase[32]. When all these limitations are considered, identification of those proteins phosphorylated by PKC has remained a major challenge. If the substrate of PKCα could be identified that plays a role in making human breast cells motile, it would provide a point of departure for understanding complex cellular functions such as metastasis as well as a novel target for designing new cancer drugs. Therefore, the aim of this project is to identify PKCα substrates in human breast cells and

to link the phosphorylation state of a PKCα substrate to the acquisition of the migration phenotype.

The Traceable Kinase Method: A Chemical-Genetic Approach for Identifying Protein Kinase Substrates.

In 1998, the Shokat laboratory (University of California, San Diego) introduced a chemical-genetic approach for identification of direct substrates of multiple protein kinases[33,34,35]. In this method, the kinase of interest is engineered to accept a non-natural phosphate donor substrate [γ-^{32}P]-(A*TP) that is poorly accepted by wildtype protein kinases in the cell. This design strategy requires engineering of a unique ATP binding pocket of the target kinase and synthesis of a complementary substituent on the A*TP. This unnatural pocket is created by the replacement of a conserved bulky residue with a glycine or alanine residue and the complementing substituent on ATP is created by attaching a bulky substituent at the N^6 amino group of the adenosine moiety of ATP[36,37]. The key residue in the wildtype enzyme makes close contact with ATP (Figure 2). Mutation of this residue to an alanine or glycine residue effectively allows efficient catalysis with A*TP analogues. As a result, the engineered kinase

- accepts an A*TP that is a poor substrate for all wildtype protein kinases.
- uses A*TP with high catalytic efficiency.
- exhibits reduced catalytic efficiency for the natural nucleotide substrate ATP so that, in the presence of cellular levels of ATP, the engineered kinase preferentially uses A*TP as the phosphodonor (applies to cell systems such as yeast which can be made to synthesize the [γ-^{32}P]-A*TP).

Structural and functional assessment of peptide specificity of mutant protein kinases with orthogonal ATP analogues showed that creation of a unique nucleotide binding pocket does not alter the binding site for the protein substrate[38]. This strategy was recently used to identify the direct targets of one tyrosine kinase (v-src) and two different serine/threonine kinases, c-Jun amino terminal kinase (JNK) and CDK2. An important advantage to applying this method to other protein kinases is that most kinase catalytic domains have a high degree of sequence homology (as in Figure 2) and so the relevant site used for mutagenesis in the protein kinase of interest can be identified by comparing its primary sequence to JNK, CDK2, or src kinase.

This combined chemical and genetic approach to address the issue of identifying direct substrates of protein kinases offers a novel and open-ended approach. By simple sequence alignment and mutation of this residue to alanine or glycine, this method has been applied successfully to several protein kinases[37,38] since it allows specific radiolabeling of their direct substrates in the presence of all other cellular protein kinases.

The endeavors to be described herein represent a successful application of the Traceable Kinase Method. In this work, direct substrates of PKCα are identified in MCF-10A human breast cells, and the phosphorylation of one of these new substrates is mechanistically linked to the phenotype of cell movement.

CHAPTER 2

MATERIALS

Cell culture serum, growth factors, media, PKCα polyclonal antibody, Alexa fluor (594 or 488)-conjugated secondary antibodies, and DNA sequencing primers were purchased from Invitrogen, Inc. (Carlsbad, CA). Antisera for PKCα, protein A/G-agarose beads and chemiluminescent reagents were obtained from Santa Cruz Biotechnology, Inc. (Santa Cruz, CA). FLAG-tag mouse monoclonal antibody, the GFP vector, anti-hrGFP, QuikChange mutagenesis reagents, and pCMV4 vector were purchased from Stratagene (La Jolla, CA). Duracryl was obtained from Genomic Solutions (Ann Arbor, MI). Immobilon-P transfer membranes were obtained from Millipore Corp. (Bedford, MA). Agarose-conjugated FLAG M-2 antibody (E-Z view beads), phosphatase inhibitor cocktail, protease inhibitors, NDPK, and anti-α-tubulin, were obtained from Sigma-Aldrich (St. Louis, MO). ^{25}Ser peptide (RFARKGSLRQKNV) was custom synthesized by GenScript Corporation (Piscataway, NJ). Fugene 6 was acquired from Roche Applied Science (Indianapolis, IN), Gelcode Blue was purchased from Pierce Co. (Rockford, IL), N^6-phenyl-ADP and N^6-phenyl-ATP analogues were purchased from Axxora (San Diego, CA), and [γ-^{32}P]-GTP was acquired from Perkin-Elmer Life and Analytical Sciences (Boston, MA). A plasmid containing the α6-tubulin cDNA insert was obtained from ATCC (Manassas, VA). Recombinant human GST(mu)-α6-tubulin was purchased from Abnova Corp. (Taiwan), GST-PKCα and β-actin antibody were obtained from Cell Signaling Technology (Beverly, MA), and GST-mu standard protein was purchased from Alpha Diagnostic International, Inc. (San Antonio, TX).

METHODS

Cell Culture and Transfection

MCF-10A human breast cells were cultured in DMEM/F-12 media supplemented with 15% equine serum, insulin (10 μg/ml), cholera toxin (100 ng/ml), epidermal growth factor (20 ng/ml), hydrocortisone (0.5 μg/ml), penicillin (100 units/ml), streptomycin (100 units/ml), and fungizone (0.5 μg/ml). MDA-MB-231 and MDA-MB-468 cells were cultured in Iscove's media supplemented with 5% FBS, penicillin (100 units/ml), streptomycin (100 units/ml), and fungizone (0.5 μg/ml) and RPMI media supplemented with 10% FBS, glutamine, penicillin (100 units/ml), streptomycin (100 units/ml), and fungizone (0.5 μg/ml) respectively. Cells were passaged at 1:6 every 3-4 days.

Transient transfection of pCMV4 vectors bearing wildtype (WT) PKCα, WT α6-tubulin or related mutants were carried out using Fugene 6 plus 4 μg of plasmid in serum free medium in the absence of antibiotics. After 6-h incubation at 30 ^{0}C, 5% CO_2, 5% serum was added, and following 48 h, transfected cells were harvested.

Mutagenesis

The cDNAs of bovine PKCα or human α6-tubulin was subcloned into pCMV-4A vector which encoded PKCα or α6-tubulin fused to a carboxy-terminal FLAG tag (DYKDDDDK). Appropriate mutants were prepared using the QuikChange site-directed mutagenesis kit (Stratagene) and two primers for each mutant consisting of a forward and its complement targeted to the region of interest. All forward primers are given in Table 1.

Mutant	Primers
PKCα-M417G	5'-GAC CGG CTG TAC TTC GTC GGC GAG TAC GTC AAC GGC-3'
PKCα-M417A	5'-GAC CGG CTG TAC TTC GTC GCG GAG TAC GTC AAC GGC-3'
α6-Tubulin-S158D	5' – GAA CGT CTC GAC GTT GAT TAT GGC AAG AAG TCC AAG CTG GAG – 3'
α6-Tubulin-S165D	5' – CGT CTC TCA GTT GAT TAT GGC AAG AAG GAC AAG CTG GAG TTC TCC – 3'
α6-Tubulin-S165N	5' – CGT CTC TCA GTT GAT TAT GGC AAG AAG AAC AAG CTG GAG TTC TCC – 3'
α6-Tubulin-S241D	5' – GTG TCC TCC ATC ACT GCT GAC CTG AGA TTT GAT GGA GC – 3'
α6-Tubulin-T337D	5' – GCC ATT GCC ACC ATC AAA GAC AAG CGT ACC ATC CAG – 3'

Table 1. Oligonucleotide primers used for site directed mutagenesis.

GFP was fused to the WT and mutant constructs of α6-tubulin and subcloned into the pCMV-4A vector (Stratagene). To confirm the presence of mutation, the entire open reading frame was sequenced for each construct (North Shore University Hospital Core Facility or Macrogen Inc.).

Cell Lysis and Western Blot Analysis

Transfected cells were harvested by trypsinization followed by three washes with complete medium. Cells were lysed by sonication (3 X 10 sec) in lysis buffer [50 mM Tris (pH7.4), 5 mM EDTA, 5 mM EGTA, 15 mM β-mercaptoethanol, and 1.0% TX-100] containing protease inhibitors (1 mM phenylmethylsulfonyl fluoride, 10 μg/mL leupeptin, 10 μg/mL aprotinin). Total protein content was determined using Bio-Rad protein reagent and BSA as a standard. Samples of equivalent protein content were applied to an 8% polyacrylimide gel and subjected to electrophoresis. Proteins were transferred to a transfer membrane. The blot was blocked with 5% milk overnight and immunochemical analysis for PKCα and a6-tubulin was carried out for PKCα by using mouse monoclonal anti-FLAG antibody, and for α6-tubulin by either anti-GFP antibody or anti-α-tubulin. For detection, the appropriate horseradish peroxidase-conjugated secondary antibody was used.

Synthesis and isolation of [γ^{32}-P]-N^6-phenyl-ATP

Radioactive phosphate was introduced at the γ-position of commercially available N^6-phenyladenosine diphosphate (N^6-phenyl-ADP, 0.833 mM, (Axorra, San Diego, CA) by using [γ-^{32}P]-GTP (250 μCi, Perkin Elmer) in the presence of bovine nucleoside diphosphate kinase (NDPK, 0.02 units, Sigma Co., St.Louis, Mo) in the medium containing 20 mM Tris (pH 7.4), 5 mM EDTA, and 1 mM DTT. The product [γ-^{32}P]-N^6-phenyl-ATP was isolated by HPLC using a Vydac quarternary amine anion exchange column. The mobile phase consisted of the following: A = NaH_2PO_4/$NaHPO_4$ (1:1 molar

ratio) at 50 mM in water adjusted to pH 2.8 with acetic acid; B = $NaH_2PO_4/NaHPO_4$ (1:1 ratio) at 250 mM, adjusted to pH 2.9 with acetic acid. The gradient started at 0% B for 2 minutes, then ramped to 60% B, followed by a linear gradient from 60-100% B for 20 min, and held at 100% B for 50 min. The flow rate was 2.0 mL/min, and peak detection was carried out at 288 nm. The moderately broad peak corresponding to [γ-^{32}P]-N^6-phenyl-ATP typically eluted between 51-57 min. This radioactive product was shown to

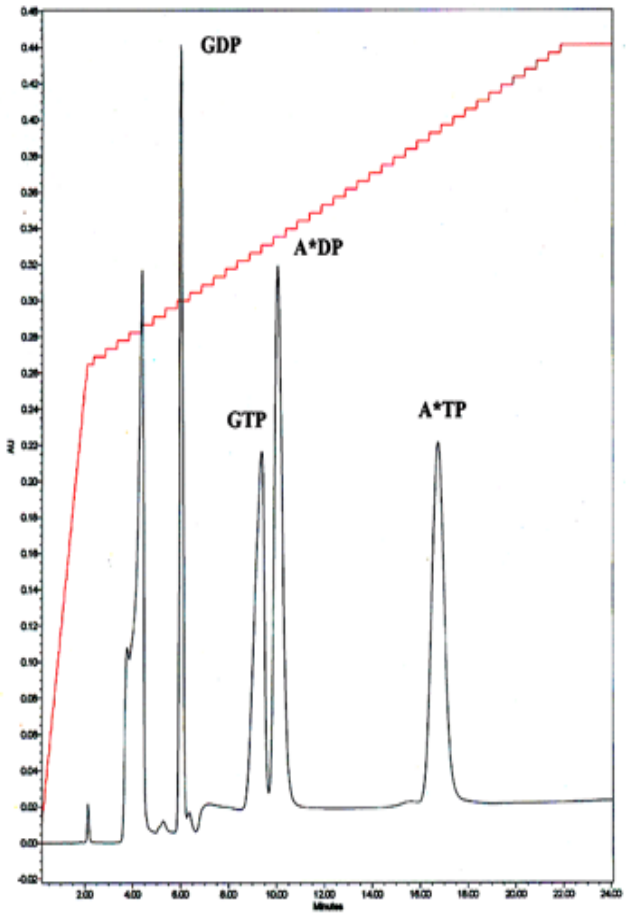

Figure 5. Separation of non-radioactive N^6-phenyl ATP (A*TP) by HPLC. (Chromatogram provided by Prof. S. A. Rotenberg)

co-elute with authentic, non-radioactive N^6-phenyl-ATP standard (Figure 5). Peak material was immediately neutralized to pH 7 with 10N NaOH. On the day of each experiment, non-radioactive N^6-phenyl-ATP was added to produce a working solution of 100μM with a typical specific radioactivity of 600-850 cpm/pmole.

PKCα catalytic activity assay *in vitro*

Lysates were prepared by sonication from transfected MCF-10A cells in the presence of hypotonic buffer [20 mM Tris (pH 7.4), 2 mM EGTA, 2 mM $MgCl_2$, 1 mM DTT], containing protease and phosphatase inhibitors. Lysates were subjected to immunoprecipitation (IP) with agarose-linked anti-FLAG antibody for 2 h at 4°C. Immunocomplexes were collected by centrifugation at 8000xg at 4°C for 30 sec. Pellets were washed twice with lysis buffer and a third wash was carried out with 2X kinase buffer [100mM Tris (pH 7.4), 1.0 mM $CaCl_2$, 20 mM MgAc, 1 mM DTT, protease inhibitors and phosphatase inhibitors]. The PKC activity assay was conducted with the IP pellet using a synthetic peptide [^{19}RFARKG<u>S</u>LRQKNV^{31}] that represents a modification (Ala^{25} → Ser) of the pseudosubstrate region in PKCα. Transfer of ^{32}P from [γ^{32}-P]-ATP or [γ^{32}-P]-A*TP to the synthetic peptide was analyzed in the presence of phosphatidylserine 0.083 mg/mL). Each reaction was quenched by applying a 50 μL aliquot to a 2 cm x 2 cm square of phosphocellulose paper that was immediately dropped into 1 L beaker of tap water. After all of the reactions had been quenched, the papers were washed five times with water, and each paper was analyzed by β-scintillation counting.

Radiolabeling of co-immunoprecipitated proteins

MCF-10A cells were transfected with WT-PKCα, M417A-PKCα, or the empty vector. Forty-eight hours post-transfection, cells were harvested by trypsinization followed by three washes with complete medium. Lysates were prepared in hypotonic buffer. WT-PKCα or mutant PKCα was immunoprecipitated using anti-FLAG agarose beads. Pellets were washed twice with IP buffer and the third time with kinase buffer, as described above. The radiolabeling reaction was carried out in the presence of kinase buffer with phosphatidylserine (0.083 mg/mL), and [γ-^{32}P]-N^6-phenyl-ATP (42 μM) for 30 min at 30^{o}C**.** The reaction was stopped by adding sample buffer and heating at 95^{o}C for 5 min. Phosphorylated products were resolved by SDS-PAGE on an 8% Duracryl gel stained with Gelcode Blue. The gel was dried and auto-radiographed for two weeks at -20^{o}C. The bands were excised and analyzed by mass spectrometry.

Radiolabeling of intracellular PKCα substrates

MCF-10A cells were transfected with WT PKCα, M417A-PKCα, or the empty vector and the cells were treated for 5 min with saponin (50 μg/mL) in sucrose buffer [130 mM sucrose, 30 mM KCl, 30 mM potassium acetate, 20 mM HEPES (pH 7.4), and phosphatase inhibitors]. Immediately after 5 min treatment of saponin, [γ-^{32}P]-N^6-Phenyl-ATP was added to cells to a concentration of 50μM and incubated for 1 h at 30^{o}C. Cells were collected by centrifugation at 8000 x g and disrupted by sonication in lysis buffer. Lysates were immunoprecipitated with the appropriate primary antibody for 2 h followed by addition of protein A/G-agarose for 1 h. Pellets were washed three times with IP buffer.

Sample buffer was added and heated for 5 min. at 95^{o}C. The bands were resolved as described above and autoradiographed for 2 weeks at -20^{o}C.

***In vitro* radiolabeling of PKCα substrates**

The recombinant GST tagged α6-tubulin (0.5 μg) was incubated with one unit of GST-tagged PKCα in 20 μl kinase reaction buffer [100mM Tris (pH 7.4), 1.0 mM $CaCl_2$, 20 mM magnesium acetate, 1 mM DTT, protease inhibitors and phosphatase inhibitors], and the reaction was initiated by adding 30 μl of 200 μM [γ-^{32}P]-ATP. After 30 min at 30^{o}C, the reaction was stopped by adding SDS-sample buffer. Samples were heated at 95^{o}C for 5 min and loaded on 6% SDS-Duracryl gel. Gel was stained with Gelcode Blue, dried, and autoradiographed for two days at -20^{o}C.

Cell motility assay

A cell sedimentation manifold (CSM, Inc., Phoenix, AZ) was used to sediment cells in to a 10-well slide. The slides were incubated at 37^{0}C and 5% CO_2. Following incubation, the manifold was carefully removed and time-resolved images were captured by a digital camera (Moticam 2000) attached to an inverted Nikon Diaphot microscope. The extent of motility was calculated by software that measures the area for each time point.

Immunocytochemistry

The cells were grown on glass coverslips. Cells were extracted in microtubule stabilizing buffer (80 mM PIPES pH 6.8), 1 mM $MgCl_2$, 4 mM EGTA, 0.5% Triton X-100) for 30 sec followed by fixation in -20 ^{o}C methanol for 3 min. After fixation, the coverslips were rehydrated 3X in TBST (150 mM NaCl, 20 mM Tris-Cl pH 7.4, 0.1% Triton X-100) for 5

min. Coverslips were blocked in antibody diluent (2% BSA, and 0.1% azide in TBST) for 10 min and treated with primary antibody (1:300) for 30 min. The coverslips were washed 3X with TBST and treated with secondary antibody (1:300) for 30 min, following which they were again washed 3X with TBST. After a quick dip in water, the coverslips were drained, mounted, and sealed.

CHAPTER 3

IDENTIFICATION OF PKCα SUBSTRATES

Identification of Site of Mutation and Synthesis of an Active Site Mutant (ASM) of PKCα

Due to similarities in the chemistry performed by all protein kinases, the example of v-src, the enzyme used by the Shokat group, provides an important model on which to re-design the PKC active site. Alignment of the primary sequences for v-src, PKA, and PKCα (shown below) revealed that the Ile residue mutated by Shokat in v-src (I-338), aligns with Met-417 in PKCα, whereas in PKA, a close relative of PKC, it aligns with Met-120. Since an x-ray crystal structure is available for the catalytic subunit of PKA that was co-crystalized with ATP, modeling studies confirmed that Met-120 makes close contact with the N^6-amino of ATP (Figure 6). From the recently published crystal structure of PKCθ [39], it was also possible to confirm that Met-417 does indeed lie within the ATP binding site of PKC (Figure 2).

v-src	(333) P-I-Y-I-V-**I**-E-Y-M-S-K (343)
PKA	(115) N-L-Y-M-V-**M**-E-Y-V-P-G (125)
PKCα	(412) R-L-Y-F-V-**M**-E-Y-V-N-G (423)
M417G	(412) R-L-Y-F-V-**G**-E-Y-V-N-G (423)
M417A	(412) R-L-Y-F-V-**A**-E-Y-V-N-G (423)

Mutant forms of PKCα in which Met-417 was substituted with either alanine (M417A) or glycine (M417G) were prepared by a standard PCR protocol, and confirmed by DNA

sequencing (North Shore University Hospital Core Facility). The mutant cDNA constructs were sub-cloned into a pCMV4 plasmid that confers a FLAG epitope tag on the expressed protein.

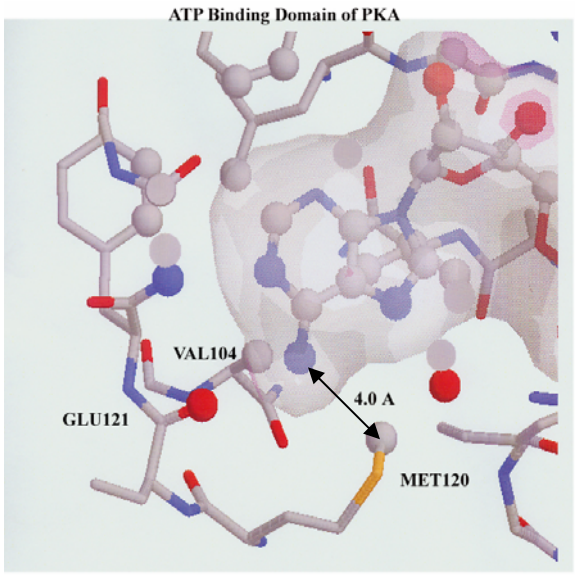

Figure 6. **X-ray crystal structure of PKA catalytic domain**. The distance between the terminal methyl group of the Met-120 sidechain is 4.0 Å from the N^6-amino group of the adenosine moiety (double-headed arrow). The ATP molecule is bounded by a translucent surface.

Characterization of PKCα Mutants in MCF-10A Human Breast Cells

Plasmids containing cDNA encoding the active site mutants were transiently transfected into MCF-10A cells. Analysis of whole cell lysates followed by Western blot analysis with anti-FLAG antibodies, demonstrates a high level of mutant expression, as shown in Figure 7.

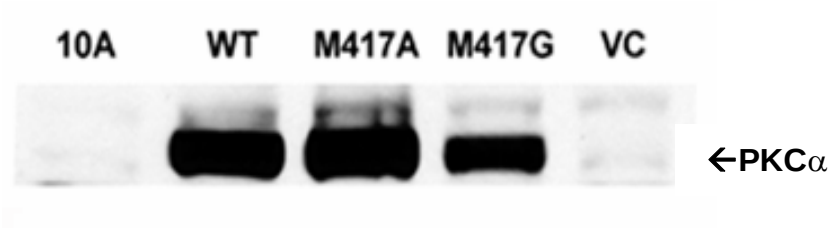

Figure 7. **Western blot analysis of FLAG-tagged mutants.** Expression levels of FLAG-tagged wildtype (WT) and mutant proteins of PKCα (80 kDa) as compared with the vector control (VC), and parental MCF-10A cells (10A). The analysis was carried out with anti-FLAG antibody.

Previous work from the Rotenberg laboratory showed that when MCF-10A cells were engineered to over-express WT-PKCα, cell motility increased[15]. To determine if each active site mutant of PKCα was competent in reproducing this phenotype, motility assays were carried out. Figure 8 reveals that both mutants induced motility but that the M417A mutant was superior to the M417G mutant, producing a level of motile behavior that paralleled that induced by the WT enzyme. This finding with transiently transfected cells reproduced the effect of WT-PKCα that had been previously demonstrated in stable transfectants of MCF-10A cells[14]. In reproducing a cell phenotype previously ascribed to WT-PKCα expression in these cells, these experiments provide compelling evidence that the M417A mutant is competent to select the same intracellular substrate(s) as the WT enzyme.

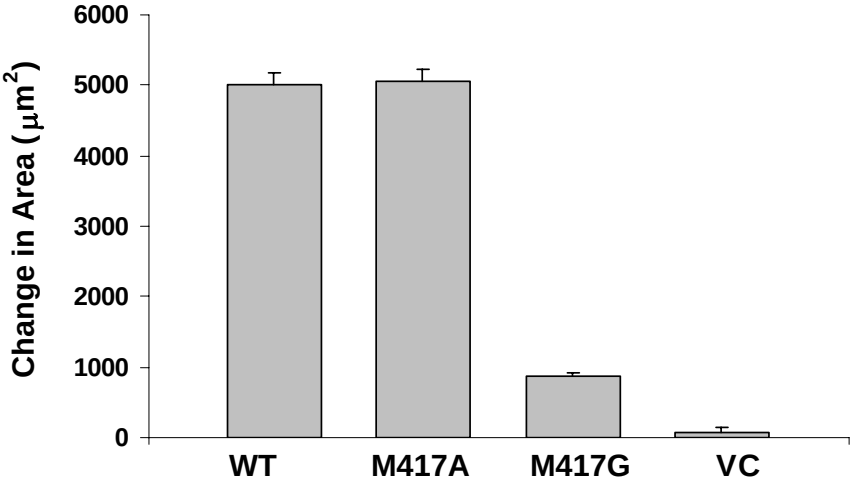

Figure 8. **Intracellular competence of PKCα mutants to engender motility of MCF-10A cells.** MCF-10A cells were transfected with wt PKCα or active site mutants (M417A or M417G). Cell motility assay was performed 48 hour post-transfection.

Selection of an ATP Analogue

To identify the optimal pairing between the active site mutant of PKCα and an ATP analogue, each mutant was screened with a commercially available panel of ATP analogues (Figure 9). Following its immunoprecipitation with anti-FLAG from transfected cells, the catalytic activity of mutant M417A was measured by testing the transfer of the γ-phosphate from [γ-^{32}P]-ATP to the ^{25}Ser peptide. The ability of each non-radioactive analogue to compete with [γ-^{32}P]-ATP was determined. The results, shown in Figure 10, indicate that all four ATP analogues were able to compete well with [γ-^{32}P]-ATP, and thus indicated that each analogue could bind to the ATP binding site. However, this experiment did not establish whether any of the ATP analogues were capable of supporting phosphoryl transfer to a substrate.

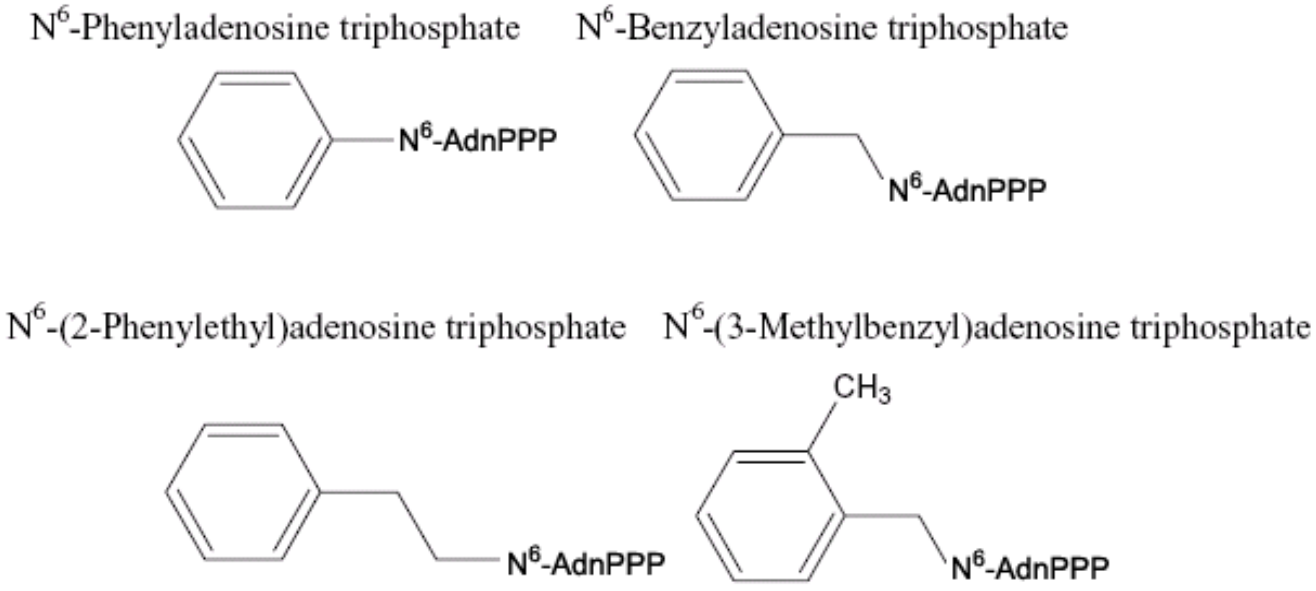

Figure 9. Commercially available N^6-ATP analogues

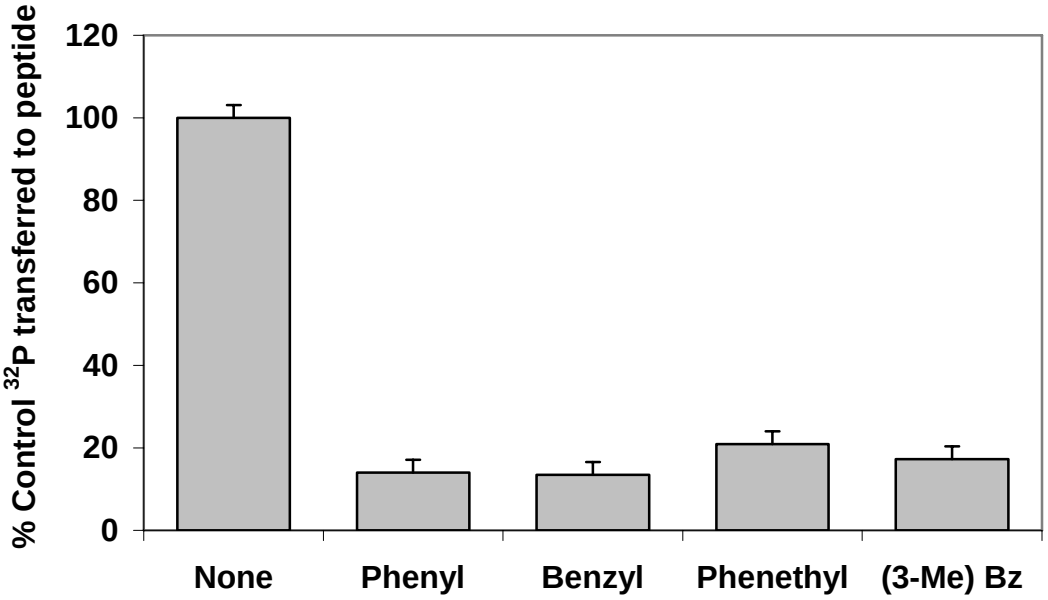

Figure 10. Competition between ^{32}P-ATP and A*TP for M417A. FLAG-M417A plasmid was transfected into MCF-10A cells. FLAG-M417A was immunoprecipitated, and was aliquoted into five sets of triplicate kinase reactions. Kinase reactions were performed with peptide substrate, 10 μM ATP, 10 μCi [γ-^{32}]-ATP, in the presence of 100 μM ATP analogue or absence. From left: no addition, N^6-phenyl-ATP, N^6-benzyl-ATP, N^6-phenethyl-ATP, and N^6-(3-methyl)-benzyl-ATP. The reactions were performed at 30 ^{o}C for 10 min, as described in the 'Methods' section.

In order to judge the ability of each non-radioactive N^6-ATP analogue to support phosphorylation of a protein substrate, assays of myelin basic protein (MBP) phosphorylation were conducted non-radioactively and analyzed by western blot with an antibody that specifically recognizes phospho-Ser at the consensus site of phosphorylation for PKC (PKC substrates antibody). As shown in Figure 11, MBP phosphorylation (18 kDa band) by the mutant PKCα was best supported by the phenyl and benzyl analogues, whereas the phenethyl derivative was completely ineffective. Therefore, the phenyl analogue was adopted for further studies with the PKCα mutant.

Figure 11. Phosphorylation of an artificial substrate (myelin basic protein) by WT-PKCα or M417A-PKCα with different N^6-ATP analogues. FLAG-PKCα plasmids (WT or M417A-PKCα) were transfected into MCF-10A cells and immunoprecipitated with anti-FLAG antibody, aliquotted into eppendorf tubes and used in a kinase reaction with myelin basic protein (MBP) plus non-radioactive 100 μM ATP analogue. ATP analogues consisted of (from left): N^6-phenyl-ATP, N^6-benzyl-ATP, N^6-phenethyl-ATP, and N^6-(3-methyl)-benzyl-ATP. The reactions were incubated at 30°C for 10 min, resolved by SDS-PAGE, and transferred to a PDVF filter. The membranes were probed with an antibody that recognizes phosphorylated PKC substrates. Protein standards consisted of non-phosphorylated MBP (MBP) and phosphorylated MBP (P-MBP).

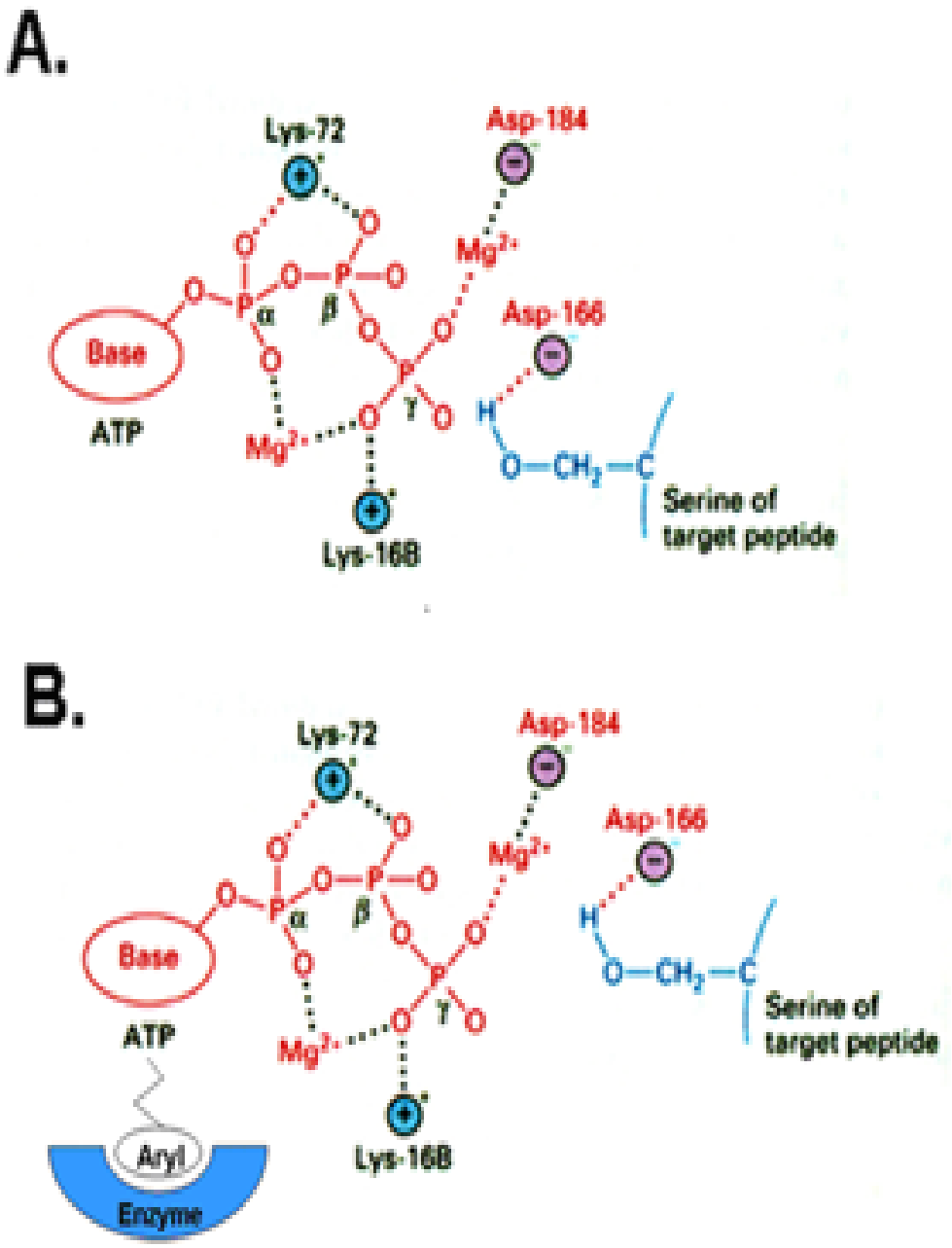

Figure 12. **Model depicting the productive and non-productive interaction between ATP and substrate.** (A) Normal productive interaction between phospho-donor and acceptor (serine residue). [B] Non-productive interaction between N^6-phenethyl-ATP and substrate due to enhanced binding of the phenyl-bearing adenosine that produces a distorted geometry between the phospho-donor and acceptor.

The finding that the catalytic activity of WT-PKCα was not supported by any of the analogues is consistent with the premise for the Traceable Kinase Method in that no N^6-substituted analogue should be accommodated by the limited space of the natural ATP binding site. In contrast, the increased space afforded by substituting Ala for Met-417 (M417A-PKCα) led to productive binding of the phenyl and both benzyl analogues. The problem encountered by the phenethyl analogue is apparently not simply a case of non-binding since its competition with ^{32}P-ATP could be demonstrated (Figure 10). The absence of phospho-transfer from the phenethyl derivative may be understood by the increased distance between the adenosine moiety and the bulky aromatic group. We speculate that, unlike the shorter linkers, the increased distance of the phenethyl analogue enables the aryl moiety to make more substantial contact with the enzyme, leading to distortion of the ATP analogue such that its geometry with the phospho-acceptor is impaired. As a result, transfer of the phosphoryl group does not occur. This model is depicted in Figure 12.

Synthesis and Testing of a Radioactive A*TP Analogue

Having identified the optimal N^6-ATP derivative for use with the PKCα mutant, the radioactive form of this analogue was prepared. Nucleoside diphosphate kinase (NDPK) generates nucleoside triphosphates from their respective diphosphates[40]. Therefore, non-radioactive N^6-phenyl-ADP was mixed with [γ-^{32}P]-GTP in the presence of NDPK to produce [γ-^{32}P]-N^6-phenyl-ATP (A*TP), as described in the 'Methods'.

$$\text{[}\gamma\text{-}^{32}\text{P]-GTP} + \text{A*DP} \xleftrightarrow{\text{NDPK}} \text{GDP} + \text{[}\gamma\text{-}^{32}\text{P]-A*TP}$$

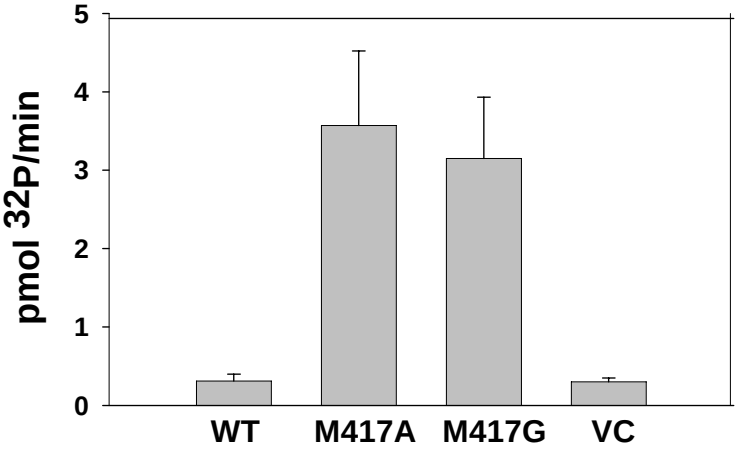

Figure 13. **Utilization of [γ-^{32}P]-N^6-phenyl-ATP.** Cells that were transfected with plasmids wt PKCα, M417A and M417G or VC were immunoprecipitated with anti-FLAG-agarose conjugate. Immunopellets were analyzed in triplicate for phosphotransferase activity with ^{25}Ser peptide and 42 μM [γ-^{32}P]-N^6-phenyl-ATP.

Following preparation of [γ-^{32}P]-N^6-phenyl-ATP, the catalytic activity of the M417A mutant with the synthetic peptide substrate was compared with that of the M417G mutant. In Figure 13, both mutants were observed to utilize [γ-^{32}P]-N^6-phenyl-ATP at an equivalent level, whereas the catalytic activity of the WT-PKCα was only slightly higher than the vector control. This result was qualitatively similar to what was found with the non-radioactive N^6-phenyl-ATP in phosphorylation of MBP by M417A (Figure 11). Therefore, these findings demonstrate that substitution of Met-417 with either Ala or Gly is sufficient to endow the enzyme with an ability to bind and utilize the N^6-phenyl-ATP analogue, and thus constitutes a proof of principle.

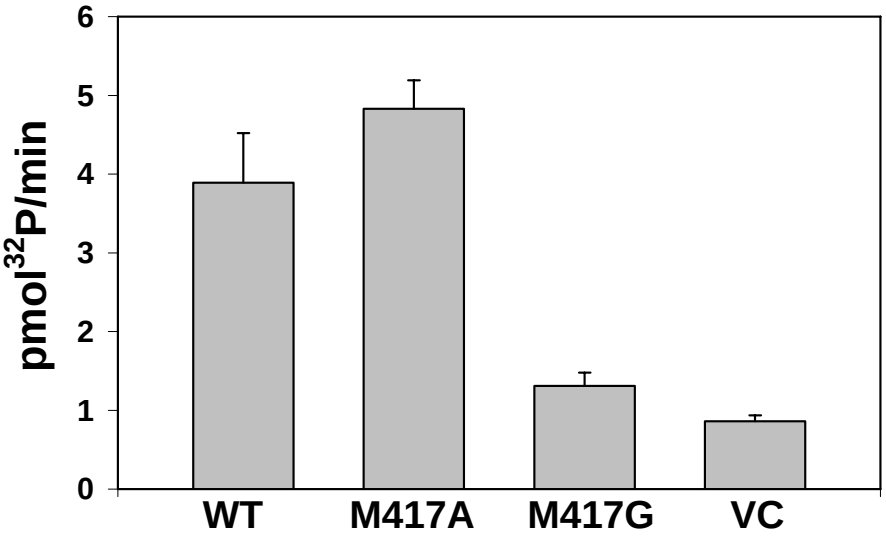

Figure 14. **Utilization of natural ATP.** *In vitro* catalytic activity of immuno-precipitated WT PKCα, mutant proteins (M417G, M417A) or vector control (VC) were assayed in triplicate with the ^{25}Ser synthetic peptide and 42 μM of [γ-^{32}P]-ATP.

While they were similar in utilizing N^6-phenyl-ATP, the two mutants exhibited a big difference in their ability to process traditional ATP. The M417A mutant exhibited significantly higher activity than the M417G mutant, and was equivalent to or exceeded the activity of the WT enzyme (Figure 14). This finding provides a plausible explanation for the observed difference in intracellular competence of each mutant (Figure 8) for which there was only ATP available.

Determination of Kinetic Constants

The values for apparent K_m and V_{max} of WT-PKCα and M417A were determined from measurements of the initial rates of transfer of ^{32}P from [γ^{32}-P] ATP or [γ^{32}-P] N^6-phenyl-ATP in the presence of activating cofactors (Ca^{2+} and PS) to the ^{25}Ser peptide at different

concentrations of ATP or N^6-phenyl-ATP. Kinetic constants were calculated from linear double reciprocal plots[41,42], as shown in the figures given below. The experimental results were obtained from two independent experiments and the kinetic constants were averaged.

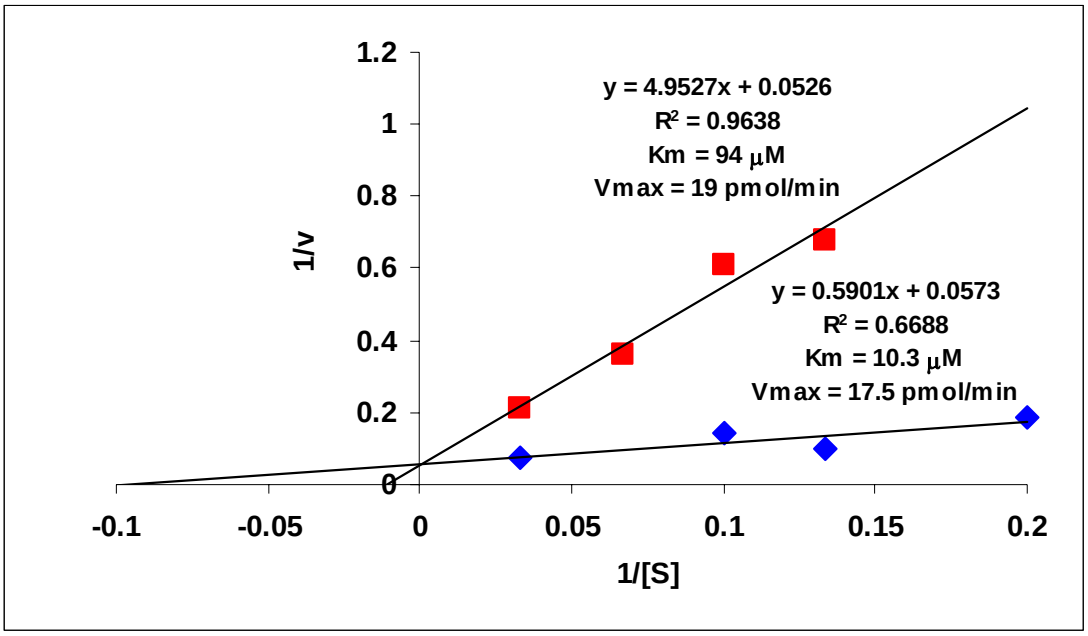

Figure 15. **Kinetic analysis of natural [γ-^{32}P]-ATP with M417A-PKCα.** Catalytic activities were measured with immunoprecipitated WT or the M417A mutant in triplicate 10 min assays at 30°C consisting of kinase buffer, ^{25}Ser peptide as substrate, and [γ-^{32}P]-ATP. The results were corrected for background activity, averaged, and analyzed by a double reciprocal plot. A representative plot was produced with M417A-PKCα (squares) or WT-PKCα (diamonds).

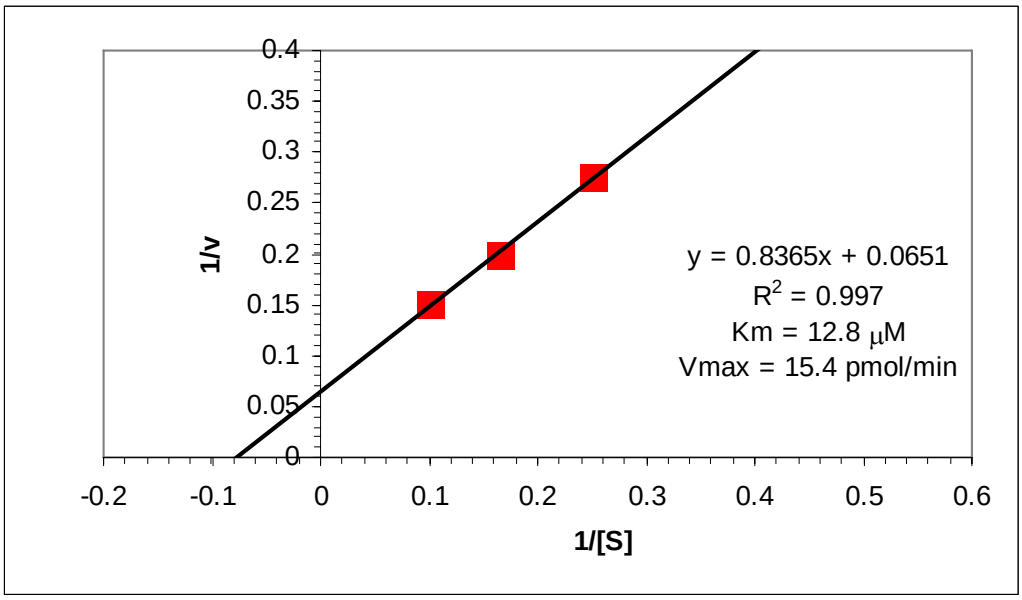

Figure 16. Kinetic analysis of [γ-^{32}P]-N^6-phenyl-ATP with M417A-PKCα. Catalytic activity was measured with immunoprecipitated M417A mutant in triplicate 10 min assays at 30°C consisting of kinase buffer, ^{25}Ser peptide as substrate, and [γ-^{32}P]-N^6-phenyl ATP. The results analyzed by a double reciprocal plot. Each data point represents the average of three measurements.

	ATP		N^6-Phenyl-ATP	
	Vmax (pmol/min)	Km (μM)	Vmax (pmol/min)	Km (μM)
Wildtype PKCα	33.5 ± 23	9.3 ± 1.5	n.d.	n.d.
M417A	30.5 ± 10	82.8 ± 11	10.3 ± 7	12.4 ± 0.4

Table 2. Kinetic constants of recombinant wildtype and mutant PKCα activities. Catalytic activities were measured with immunoprecipitated WT or M417A mutant in triplicate assays consisting of kinase buffer, ^{25}Ser peptide (32 μM), and either [γ-^{32}P]-ATP (5-30 μM) or [γ-^{32}P]-N^6-phenyl-ATP (4-10 μM). The results were corrected for background activity, averaged, and analyzed by a Lineweaver-Burk plot (examples of which are given in Figures 15 and 16). Each value shown is the average of two independent experiments. [n.d., not determined]

As shown in Table 2, K_m = 9.3 μM for ATP with WT-PKCα while for M417M, K_m = 82.8 μM; both enzymes exhibited similar V_{max} values with ATP. Therefore, the mutant PKCα exhibited weaker binding with traditional ATP but within the physiological range of the cell. The reported K_m for ATP for rat brain PKC α/β isoforms was 24 μM with the same peptide substrate[43] However, with N^6-phenyl-ATP, the M417A mutant exhibited K_m = 12.4 μM, and was therefore equivalent to the affinity of WT PKCα for ATP (K_m = 9.3 μM). These values demonstrate that the M417A mutant binds N^6-phenyl-ATP with high affinity and carries out phosphoryl transfer at a rate that is comparable to that of the WT enzyme with traditional ATP.

Radiolabeling of Immunoprecipitated PKCα-associated Proteins

To identify direct substrates of PKCα, the method that proved to be the most effective in producing ^{32}P-labeled products was to co-immunoprecipitate M417A-PKCα from MCF-10A cells whereby high affinity substrates would be "pulled down" with the enzyme. Subsequently, these substrate proteins were subjected to phosphorylation upon addition of [γ–$^{-32}$P]-N^6-phenyl-ATP. An alternative method that was not as effective (results not shown) was to immunoprecipitate M417A-PKCα and add to it a virgin cell lysate (containing all substrate proteins) and [γ–$^{-32}$P]-N^6-phenyl-ATP.

From the first method, radioactive products were resolved on SDS-PAGE, stained with Gelcode blue and subjected to autoradiography for two weeks (Figure 17). There was a noticeable difference in the pattern of labeled substrates between reactions with WT-PKCα and M417A-PKCα. However, background phosphorylation with WT-PKCα was

detected. The possible sources of this background will be examined in the 'Discussion'. In a representative experiment shown in Figure 17, the strong bands unique to M417A-PKCα were excised from the gel and submitted for analysis by mass spectrometry. The proteins that were identified from these selected bands are given in Table 3.

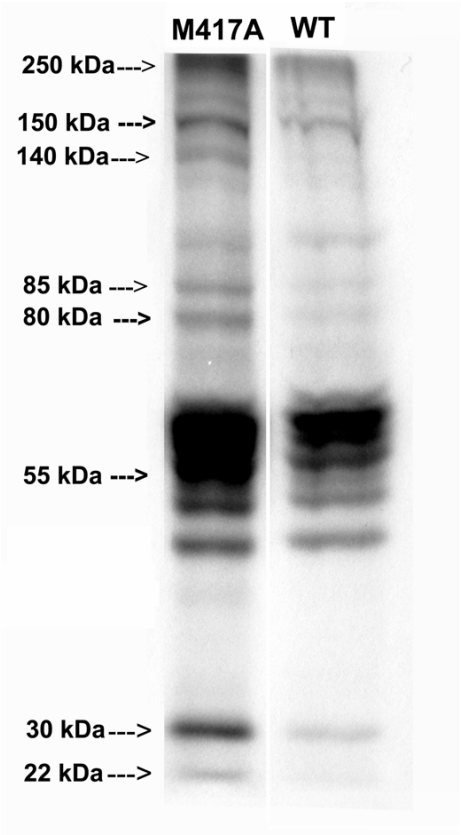

Figure 17. ***In vitro*** **phosphorylation of protein substrates co-immunoprecipitating with M417A or WT-PKCα.** In triplicate tubes containing immunopelleted M417, reactions were initiated by addition of [γ-^{32}]-phenyl-ATP and the reaction progressed for 30 min at 30^{o}C and thereafter was quenched by addition of sample buffer and heating at 95^{o}C for 5 min. The samples were resolved by 8% SDS-PAGE, dried on blotting paper, and auto-radiographed for two weeks at -20 ^{o}C.

Candidate Substrates of PKCα Identified by Mass Spectrometry

Molecular Mass (kDa)	Protein
~15	Histone H2A, Histone H3 (*in vitro PKC substrate)*
~50	Eukaryotic translation elongation factor 1-α1 (eEF-A1) (intracellular PKC substrate)
~55	α6-tubulin
~69	LaminA/C (intracellular PKC substrate)
~70	Ku70
~85	Hsp 90

Table 3. Proteins identified by mass spectrometry as potential PKCα substrates.

Identification of known PKC substrates confirms the reliability of this method. Among these proteins, histone H2A/H3, eEF-A1, and lamins A and C were all known to be PKC substrates, whereas the other identified proteins are potentially novel PKC substrates. Their validation must include an in-depth analysis of the impact of phosphorylation on their intracellular function.

Histones are protein components of chromatin. Six major classes of histones are known and include: H1, H2A, H2B, H3 and H4. Histones are subject to post-translational modification by enzymes primarily on their N-terminal tails, but also in their globular domains. Such modifications include methylation, acetylation, phosphorylation, ubiquitination and ADP-ribosylation. These modifications affect the regulation of gene expression[44].

eEF1A is an abundant protein that constitutes 1 to 3% of the total soluble protein in the cell. eEF1A plays a central role in protein synthesis, delivering aminoacyl-tRNAs to the elongating ribosome. Like other components of the translation apparatus, this protein has functions in processes aside from elongation that include effects on viral replication, calmodulin binding, and actin bundling. At least three types of post-translational modifications have been reported for eEF1A: Lys residues are methylated, Ser residues are phosphorylated, and Glu residues are modified by the attachment of PGE[45].

It has been shown previously that histones H2/3, and EF 1 all undergo phosphorylation in vitro by PKC [46,47,48].

Lamins are intermediate filament-type proteins which form major components of the nuclear lamina, a protein network underlying the inner nuclear membrane that determines nuclear shape and size. Lamins form dimers through their rod domain and interact with chromatin and integral proteins of the inner nuclear membrane through binding sites located in their carboxy-terminal globular tail. Mammals have two main type lamins, A and B. ***B-type lamins*** B1 and B2 are encoded by two distinct genes whereas ***A-type lamins*** A and C are derived by differential splicing and alternative polyadenylation from one gene. It was previously shown that lamin C undergoes phosphorylation by PKCα at Ser 572[49].

Ku70 is one component of a protein complex, Ku70 and Ku80 that functions as a heterodimer to bind DNA double-strand breaks (DSB) repair in the nucleus and activates

DNA-dependent protein kinase[50]. Phosphorylation of Ku70 protein has not been described before and the functional consequences of Ku70 phosphorylation remain incompletely understood. Although generally studied as a DNA repair enzyme that is found in the nucleus, a recent finding that Ku70 can be found at the plasma membrane[51] suggests that PKC would have the opportunity to phosphorylate it. Its membrane-related function is at present unknown.

Heat shock protein 90 (Hsp90), an abundant molecular chaperone in the eukaryotic cytosol, is involved in the folding of a set of cell regulatory proteins and in the re-folding of stress-denatured polypeptides. The basic mechanism of action of Hsp90 is not yet understood[52]. Several small molecule inhibitors of the molecular chaperone Hsp90 have been identified over the past decade that have the unusual ability to decrease the activity of multiple receptors, kinases, and transcription factors known to be involved in human cancers[53]. This suggests that Hsp90 may undergo phosphorylation but the functional significance of this modification is unknown. Alternatively, it may be the case that the phosphorylation of Hsp90 by PKCα occurs adventitiously, i.e., that its occurrence is inconsequential, and that the co-localization of PKCα and Hsp90 (resulting in their co-immunoprecipitation) is an indication that PKCα is a client of Hsp90.

Six human α-tubulin isotypes, all of which can undergo post-translational modifications, have been detected by the reverse transcriptase-polymerase chain reaction[48]. These isotypes play a role in development and in the building of specialized microtubule-based

structures. Of the six human α-isotypes known to exist, only α6- and Kα1- tubulin have been detected in human carcinoma cancer cells[54].

Discussion

To identify novel PKCα substrates, we adopted the approach developed by Shokat and coworkers that entails mutating the ATP binding site of PKCα. This mutation was done in a way that allows it to utilize a bulky ATP analogue (N^6-phenyl-ATP). The site of mutation in the traceable kinase was identified at Met-417 since it aligned with Ile-338 in v-src, Shokat's model enzyme, and with Met-120 in PKA, a close relative of PKCα. Aided by the availability of the three dimensional structure of PKA that had been co-crystallized with ATP-Mg^{2+}, the proximity of M120 in PKA to the N^6-amino group of the adenosine moiety (Figure 6) could be directly verified. Based on this strategy, Met-417 was mutated to Ala or Gly. Both mutants expressed a high level of PKCα activity with N^6-phenyl-ATP in vitro, but intracellular signaling by M417A-PKCα (as judged from the motility phenotype) was superior to that of the M417G mutant (Figure 8). This difference in intracellular competence was later attributed to a differential ability to process traditional ATP.

To identify biologically relevant substrates, the M417A-PKCα and [γ-^{32}P]-ATP analogue were added to a whole cell lysate[55]. Addition of large quantities of a kinase to a cell lysate could result in nonspecific phosphorylation of substrates. Therefore in this study, we expressed the mutant and wild-type PKCα in MCF-10A cells and then

immunoprecipitated PKCα that effectively extracted it high affinity substrates from the complex protein mixture.

In accordance with the premise of the Traceable Kinase method, the use of [γ-^{32}P]-phenyl ATP with WT-PKCα resulted in some background incorporation of ^{32}P into proteins, while the use of [γ-^{32}P]-phenyl-ATP with the M417A mutant resulted in phosphorylation of unique bands (Figure 17). The high background of radioactivity produced by control samples deserves further comment. Although the source of the background in MCF-10A cells remains undefined, it is probably not due to co-immunoprecipitation of endogenous PKCα (via self-dimerization) since this isoform is expressed at exceedingly low levels, and its presence would have been evident in peptide-based catalytic assays of immunopellets containing either WT PKCα or vector control samples. However, these catalytic assays would not have detected in the presence of protein substrates. One plausible explanation is that immunoprecipitation with the FLAG antibody in detergent-free isotonic buffer pulls down other protein kinases that persist as nonspecifically bound proteins, despite multiple washes of the immunopellet. This possibility is supported by the increased number and intensity of radioactive bands produced with natural [γ-^{32}P]-ATP in an immunopellet isolated from vector control-treated cells (results not shown). The few high-intensity bands observed in control samples with [γ-^{32}P]-phenyl-ATP (Figure 17) suggest that there are native protein kinases that can utilize phenyl-ATP.

An alternative explanation is that the background bands could result from the reverse reaction of NDPK in the cells, which could generate [γ^{-32}P]-ATP if there were a sufficient

amount of ADP that co-immunoprecipitated. In this regard, MCF-10A cells were observed to express high levels of NDPK protein (data not shown). If there were a high enough level of [γ^{-32}P]-ATP generated by this contaminating NDPK activity, then phosphorylation would occur by co-immunoprecipitation of irrelevant protein kinases. One possible approach to suppress the activity of other protein kinases is to add nonradioactive ATP to the labeling reaction mixture along with [γ-^{32}P]-phenyl-ATP, coupled with the use of the M417G mutant, which weakly utilizes ATP and therefore would preferentially bind the radioactive ATP analogue. Another option is to use a different epitope tag such as GST whose isolation can be carried out with glutathione-agarose beads instead of an antibody. If high background signals obscure bands that are unique to the traceable mutant, then resolution of radiolabeled products by two-dimensional SDS-PAGE can be performed. Over and above these technical considerations, it should be emphasized that the high background observed here with MCF-10A cells is not likely to occur with all cell lines. Indeed, similar analyses being conducted in this laboratory with human prostate cells (LNCaP cells) produce much lower background levels.

The method developed here for the identification of novel PKCα substrates could be employed for identification of PKCα substrates in various other cell lines and tissues.

These results confirm that the traceable kinase method can be used to identify PKCα substrates. However, it may be surprising that well-defined PKC interacting proteins such as MARCKS, receptor activated C kinase (RACK), annexins, vinculin, perinuclear

binding protein-1 (PICK-1) and adducin were not detected as PKCα substrates. One reason is that only a few bands resolved by SDS-PAGE were sent for sequencing, and the other reason may be that some of these well known proteins (such as MARCKS) are not highly expressed in MCF-10A cells.

Therefore, by using the technique originally developed by Shokat and coworkers for *src*, we demonstrated the ability to modify the ATP pocket on PKCα and consequently to utilize a modified form of ATP and exhibit high affinity toward this analogue. Importantly, the modification does not hamper the kinase activity, and it does not affect the recognition of PKCα substrates in the cell, as demonstrated by the competence of the M417A PKCα mutant to reproduce the motility phenotype.

According to the Table 3, there are other proteins which had not been previously identified as PKCα substrates and thus may be significant to one or more of the phenotypes that had been previously ascribed to PKCα in MCF-10A cells. One of these proteins, α6-tubulin, is a cytoskeletal protein that serves as a component of microtubules. Because of the role of the cytoskeleton in cell movement, the possibility was pursued that α6-tubulin is a direct substrate of PKCα having physiological significance. Therefore the next goal of this project was to characterize α6-tubulin as a protein substrate of PKCα that engenders the motility phenotype.

CHAPTER 4

Phosphorylation of α6-Tubulin by PKCα Controls Motility and Microtubule Structure of MCF-10A Cells.

Microtubules comprise a major component of the cytoskeleton and play an important role in morphological changes associated with cell migration. The α and β subunits of tubulin, each approximately 50 kDa, assemble into α/β heterodimers that in turn polymerize into microtubules. A third form of tubulin (γ-tubulin) that is involved in nucleation has also been described[56]. The α and β subunits of tubulin each represents a family of isoforms that arose partly due to tubulin multigene expression and partly due to a number of post-translatiional modifications[21]. Such modifications include tyrosination, polyglutamylation, acetylation, and phosphorylation (primarily on tyrosine residues)[57]. The consequences of these post-translational modifications to tubulin function remain unknown. Some of these events are associated with stable populations of microtubules, while others seem to influence the binding of motor proteins. Recent evidence suggests that tubulin modifications may play a role in cell migration and in multi-drug resistance to chemotherapy[58]. However, there is little evidence for a role of modification in the regulation of microtubule dynamics.

PKC expression or activation is known to cause alterations in the cytoskeleton. Dramatic morphological changes result when MCF-10A cells are either treated with phorbol esters or engineered to over-express PKCα.[13]. Many of these changes arise from alterations in actin structure, although the precise molecular mechanisms remain unclear. The following evidence implicates PKC in regulating microtubule function:

- A number of microtubule-associated proteins are substrates for PKC both *in vitro* and *in vivo*[59,60].
- Phorbol esters cause microtubule reorganization[61,62].
- PKC βI has been shown to co-localize with microtubules and bind microtubule-associated proteins[62].
- PKC isoforms ε and δ have been reported to localize to the centrosome[63,64]
- PKC β-deficient T cells failed to develop a polarized microtubule network, a defect that can be rescued by expressing PKCβI[65].

Since microtubules are composed of α/β heterodimers and α-tubulin was identified as a potential substrate of PKCα (Table 3), it is possible that the effects of PKCα on cytoskeletal structure can be explained in part by its phosphorylation of α-tubulin. Two important questions are whether *intracellular* α-tubulin is indeed phosphorylated by PKCα and, if so, what are the cellular consequences of that phosphorylation?

Phosphorylation of tubulin has received very little attention. Recently, serine phosphorylation of β-tubulin was reported[66,67,68]. In that study, cdk1 kinase was demonstrated to phosphorylate β-tubulin at Ser-172 and this event was further shown to influence cell cycle characteristics. In the present study, we show that PKCα directly phosphorylates purified recombinant α6-tubulin in vitro and α-tubulin in intact MCF-10A cells, and that this phosphorylation alters microtubule structure and engenders the cell motility in these non-motile human breast cells.

***In Vitro* Phosphorylation of α6-Tubulin by PKCα**

To test directly whether PKCα phosphorylates α-tubulin, GST-tagged α6-tubulin was incubated with or without pure recombinant PKCα in the presence of [γ-^{32}P]-ATP, followed by SDS-PAGE and autoradiography. The results indicate that PKCα phosphorylates α6-tubulin (Figure 18). The coomassie blue-stained gel band corresponding to phosphorylated α6-tubulin runs a little slower when compared with non-phosphorylated α6-tubulin. These results indicate that α6-tubulin is a PKCα substrate *in vitro.*

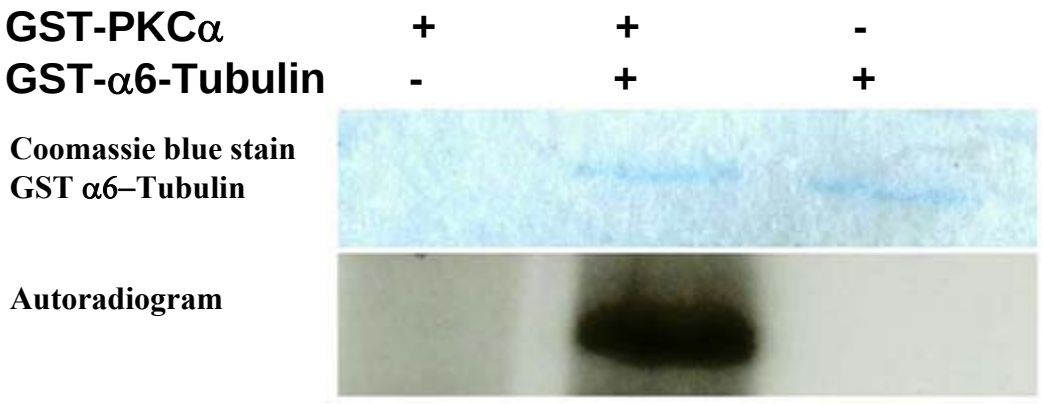

Figure 18. **PKCα phosphorylates recombinant α6-tubulin in vitro.** Direct phosphorylation of recombinant 75-kDa GST-α6-tubulin (1 μg) by recombinant GST-PKCα (1 μg), was carried out in the presence of 50 μM [γ-32P]-ATP, activating cofactors and kinase buffer for 30 min at 30 ^{o}C, as described in the 'Methods'. The products were resolved by 6% SDS-PAGE, the gel was stained with Coomassie blue,and autoradiographed at –20 ^{o}C for 2 days. The results are representative of two independent experiments.

Phosphorylation of Intracellular α-Tubulin

To phosphorylate intracellular α-tubulin, the ATP analogue ([γ-^{32}P]-N^6-phenyl-ATP) must be introduced into intact cells that express the M417A-PKCα mutant. Because cells are impermeable to ATP, the detergent saponin was used to permeabilize MCF-10A cells (Figure 19). At low concentrations, saponin permeabilizes the plasma membrane, but has little effect on internal membranes, such that many of the internal cell structures and rate of protein synthesis are undisturbed[69]. Pilot studies demonstrated that when saponin is added at a concentration of 50μg/ml, MCF-10A cells readily take up fluorescein-conjugated ATP. These cells were detectable within 5 min and remained stable for more than 3 hours following saponin treatment.

Similar conditions were adopted to permeabilize MCF-10A cells that had been transfected with cDNA encoding M417A-PKCα or the corresponding empty vector (VC). Forty-eight hours post-transfection, cells were collected using tripsin and treated with saponin (50 μg/ml) in hyptonic sucrose buffer. [γ-^{32}P]-N^6-phenyl-ATP was added to 100 μM and the cells were incubated in this medium for 1 h at 30^{o}C. Following centrifugation, the cells were lysed and immunoprecipitated with α-tubulin antibody. Immunopellets were subjected to SDS-PAGE and autoradiography. As shown in Figure 20, α-tubulin was observed to undergo phosphorylation in MCF-10A cells that express the M417A-PKCα but not in vector control cells.

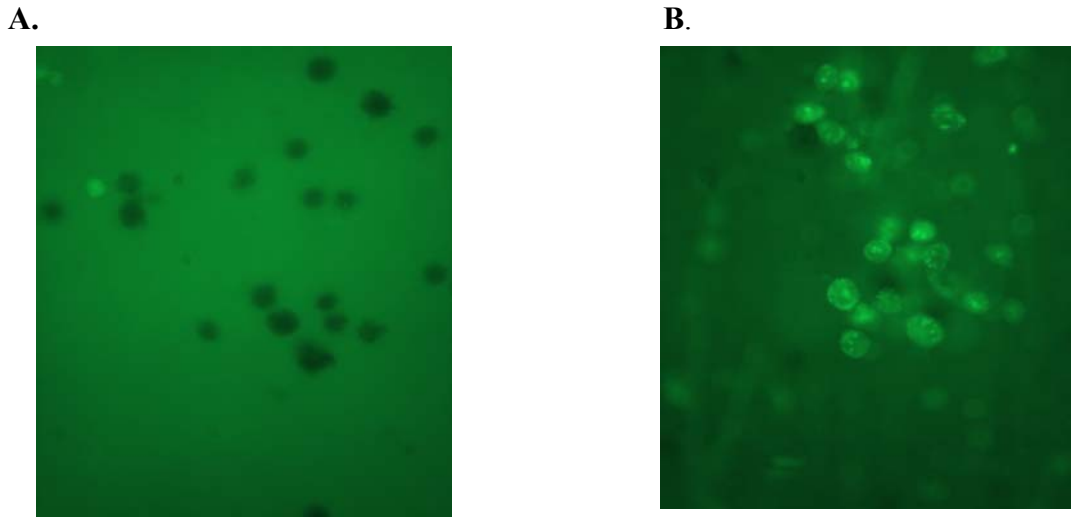

Figure 19. **Permeabilization of MCF-10A cells with the detergent saponin.** MCF-10A cells were incubated with fluorescein-conjugated ATP in the absence (A), and presence of saponin (50 μg/ml) (B).

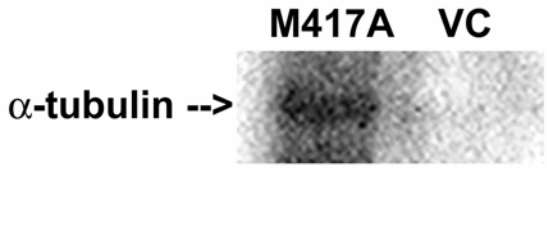

Figure 20. **Phosphorylation of α-tubulin in permeabilized MCF-10A cells that were treated with 100 μM [γ-^{32}P]-phenyl-ATP.** Cells that had been transfected with M417A-PKCα, or the empty vector (VC) were harvested and permeabilized with saponin, as described in the 'Methods'. To determine whether α6-tubulin was phosphorylated, cell lysates were immunoprecipitated with anti-α-tubulin, and the immunopellets were analyzed by SDS-PAGE and autoradiography.

Mutagenesis of Potential PKC Phosphorylation Sites in α6-Tubulin

It has been known since the mid-1980s that PKCs preferentially phosphorylate sequence motifs in which the phosphorylatable Ser or Thr residue is flanked by two or more Arg or Lys residues[70]. Inspection of the α6-tubulin primary sequence indicates that it has four PKC consensus phosphorylation sites. Sequence analysis reveals that Ser-165 and Thr-337 are strong candidates because both of them are flanked by at least two Lys residues, while the other two sites (Ser-158 and Ser-241) have a single cationic residue on only one side.

tttggtgggggaactggttctgggttcacctcgctgctcatggaacgtctctcagttgat
F G G G T G S G F T S L L M E R L S V D

tatggcaagaagtccaagctggagttctccatttacccggcgccccaggtttccacagct
Y G K K S K L E F S I Y P A P Q V S T A

tccctgagatttgatggagccctgaatgttgacctgacagaattccagaccaacctggtg
S L R F D G A L N V D L T E F Q T N L V

ggtgacgtggttcccaaagatgtcaatgctgccattgccaccatcaaaaccaagcgtacc
G D V V P K D V N A A I A T I K T K R T

(Ser-158, Ser-165, Ser-241, and Thr-337)

Human α6-tubulin was sub-cloned into the pCMV4 vector (at the BamH1 and Xho1 restriction sites) so that the expressed α6-tubulin was fused with a FLAG tag. Using site-directed mutagenesis, each potential site of phosphorylation was subjected to a single point mutation that substituted an Asp residue (D) for either Ser or Thr. This mutation effectively simulated the presence of phosphate at that position ("pseudo-phosphorylation"). For one mutant (S165D) the phosphorylation-resistant mutation was introduced by substituting Asn (N). The forward and reverse primers used for each mutant are listed in Table 1. (See 'Methods' section.) The amino terminus of these mutants and

WT-α6-tubulin was fused with green fluorescent protein (GFP) separated by a linker of six Gly codons, as shown in the schematic representation (Figure 21).

Figure 21. Schematic representation of GFP fusion of α6-tubulin.

Expression of GFP-α6 Mutants in MCF-10A cells

GFP-fused WT-α6-tubulin and related mutants were over-expressed in MCF-10A cells. Approximately 48 hours post-transfection, cells were harvested and lysates were prepared. Equivalent protein amounts (100 μg/lane) were analyzed by Western blot using hrGFP antibody to probe expression levels of α6-tubulin protein. The results revealed that WT as well as the mutant proteins were strongly expressed in MCF-10A cells (Figure 22). It is noted that these signals were strongest when the protein samples were properly solubilized in sample buffer to a final concentration of approximately 2 mg/ml.

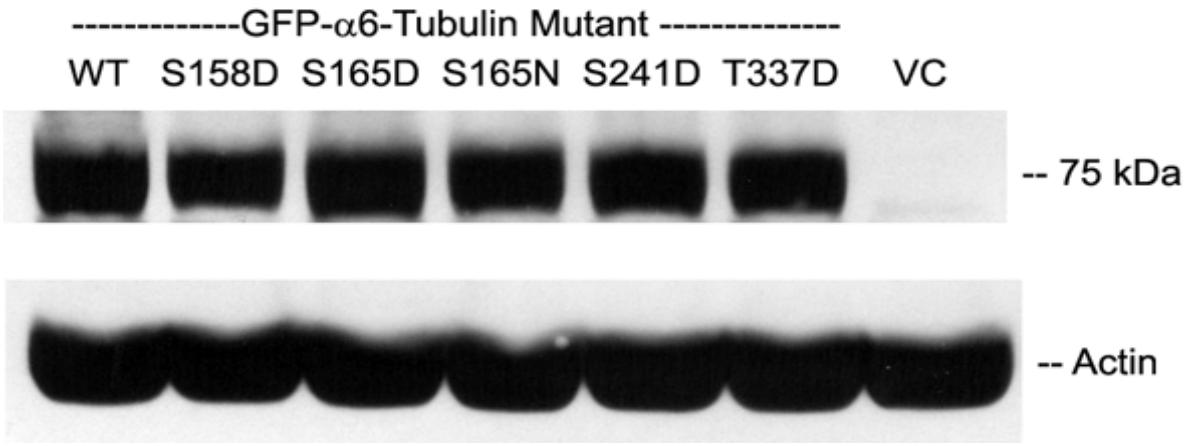

Figure 22. **Expression of wildtype and mutant α6-tubulin proteins.** Lysates from MCF-10A transfectants expressing WT or mutant hrGFP-α6-tubulin proteins were analyzed by Western blot (100μg/lane) using hrGFP monoclonal antibody. β-actin expression was used as the loading control.

Effect of Pseudo-phosphorylated α6-Tubulin Mutants on Cell Motility

To determine whether phosphorylation of α6–tubulin leads to the acquisition of motile behavior, MCF-10A cells were transfected with each α6-tubulin construct. Migration assays for each transfection was performed using a cell sedimentation manifold, as described in the 'Methods' section. As shown in Figure 23, the mutant bearing a pseudo-phosphate at Ser-165 (S165D) exhibited increased cell motility by more than three-fold as compared to WT, or any other pseudo-phosphorylated mutant (S158D, S241D, and T337D). Importantly, the increase in cell motility of S165D was comparable to the increase of motility engendered by WT-PKCα expression in MCF-10A cells (hatched bar).

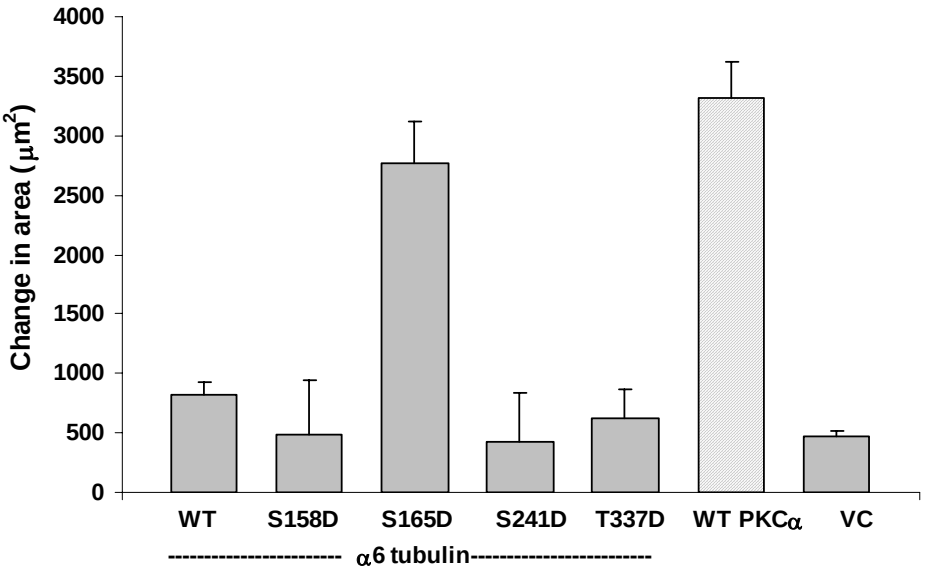

Figure 23. **Mutants of α6-tubulin and MCF-10A cell motility.** Measurement of cell motility was carried out with MCF-10A cells that had been transfected with single-site mutants of α6-tubulin (S165D, S158D, S241D, or T337D), WT PKCα, or vector control (VC). Each value is the average of triplicate measurements, and the results are representative of three independent experiments.

Effect on Motility by a Phosphorylation-resistant Mutation at Ser-165

In view of the result that the pseudo-phopshorylated mutant at Ser-165 (S165D) increased cell motility, a phosphorylation-resistant homologue was prepared in which Ser-165 was substituted with an Asn residue (S165N). Compared with MCF-10A cells that had been transfected with WT-PKCα only (which is sufficient to cause high levels of motility), a dominant-negative effect was observed in cells co-transfected with WT-PKCα and S165N (Figure 24). Similarly, in cells whose motility was activated by treatment with DAG-lactone, which activates both conventional and novel PKC isoforms, the S165N was observed to produce a similar dominant-negative effect on motility as that produced by expression of the kinase defective (KD)-PKCα mutant (Lys368 → Arg).

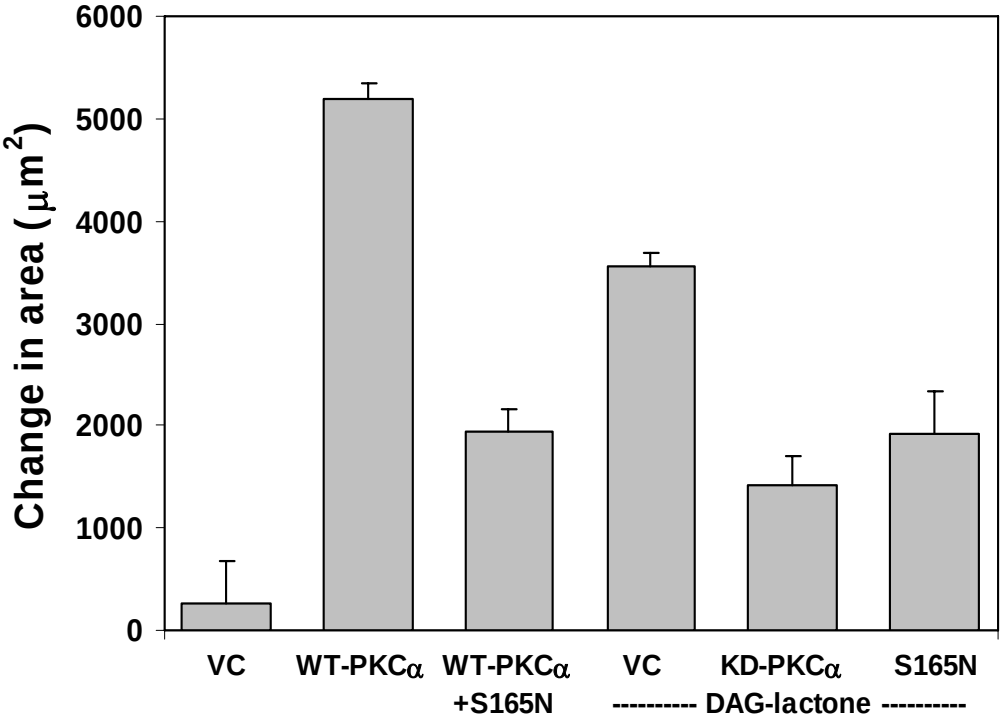

Figure 24. Expression of S165N-α6-tubulin causes a dominant negative effect on motility of MCF-10A cells. Phosphorylation-resistant α6-tubulin mutant (S165N) decreases the motile behavior of stimulated MCF-10A cells. MCF-10A transfectants expressing the S165N mutant were tested for a dominant-negative effect on motility that had been induced by either WT-PKCα over-expression or addition of 10 μM DAG-lactone.

The impact of S165N-α6-tubulin on motility was assessed with highly metastatic human breast cells, namely MDA-MB-231 cells (express high levels of PKCα), and MDA-MB-468 cells (express no PKCα). As shown in Figure 25, expression of the S165N mutant decreased the motility of both MDA-MB-231 and MDA-MB-468 cells by approximately 50% and 70%, respectively. These findings imply that α6-tubulin phosphorylation at S165 has a significant dominant-negative effect on motility of these metastatic cells that is activated by either PKCα individually or by other DAG-sensitive PKC isoforms.

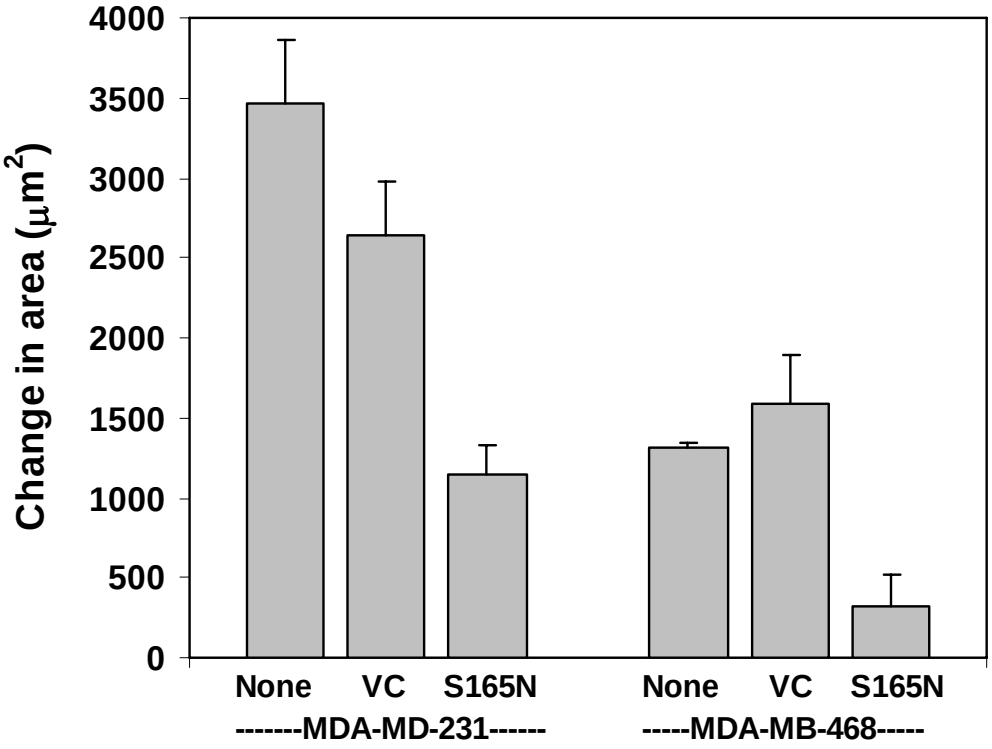

Figure 25. Expression of S165N-α6-tubulin in metastatic human breast cells causes a dominant-negative effect on motility. Dominant-negative effect of S165N on human breast tumor cell lines that express high levels of PKCα (MDA-MB-231) or none at all (MDA-MB-468). Each value is the average of triplicate measurements, and the results are representative of three independent experiments.

Effects of WT-PKCα, WT-α-tubulin, and α6-tubulin mutants on cell morphology.

Microscopic examination of WT PKCα, WT α-tubulin and all the mutants transfectants did not reveal any significant alterations in cellular morphology compared to parental cells (Figure 26).

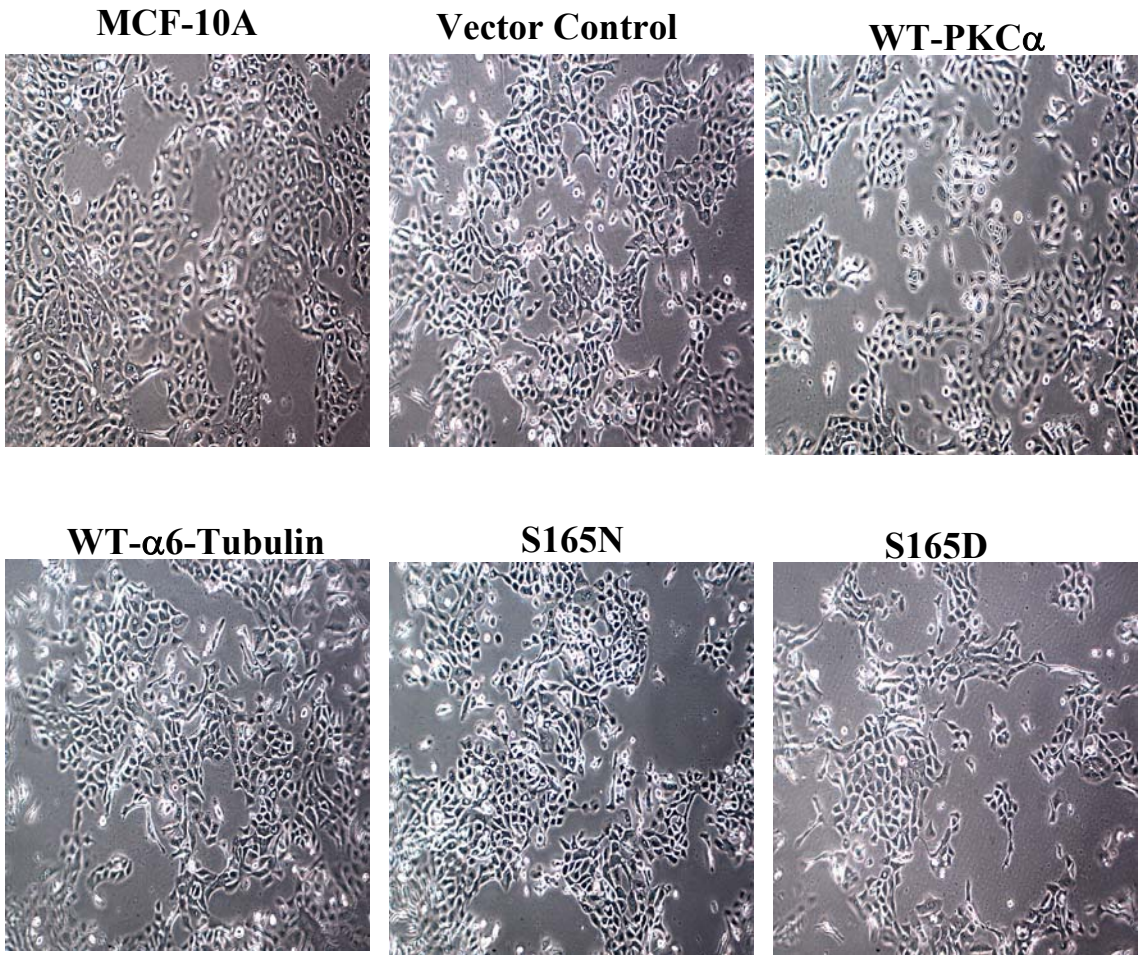

Figure 26. Morphology of MCF-10A cells transfected with WT-PKCα, WT-α6-tubulin, or related mutants. Transfected cells were visualized in brightfield by phase contrast microscopy (Nikon Diaphot).

Even though there was no significant morphological difference between control cells and PKCα transfectants, their microtubule structure showed a dramatic change (Figure 27). In contrast to the control transfectants whose microtubules consisted of highly extended structures, PKCα-transfected cells had a profoundly truncated microtubule structure. It is known that, PKCα is in the activated form when it is over-expressed in MCF-10A cells

(Sun and Rotenberg, 1999). Taken together, these findings imply that activation of PKCα in MCF-10A cells has an effect on microtubule polymerization.

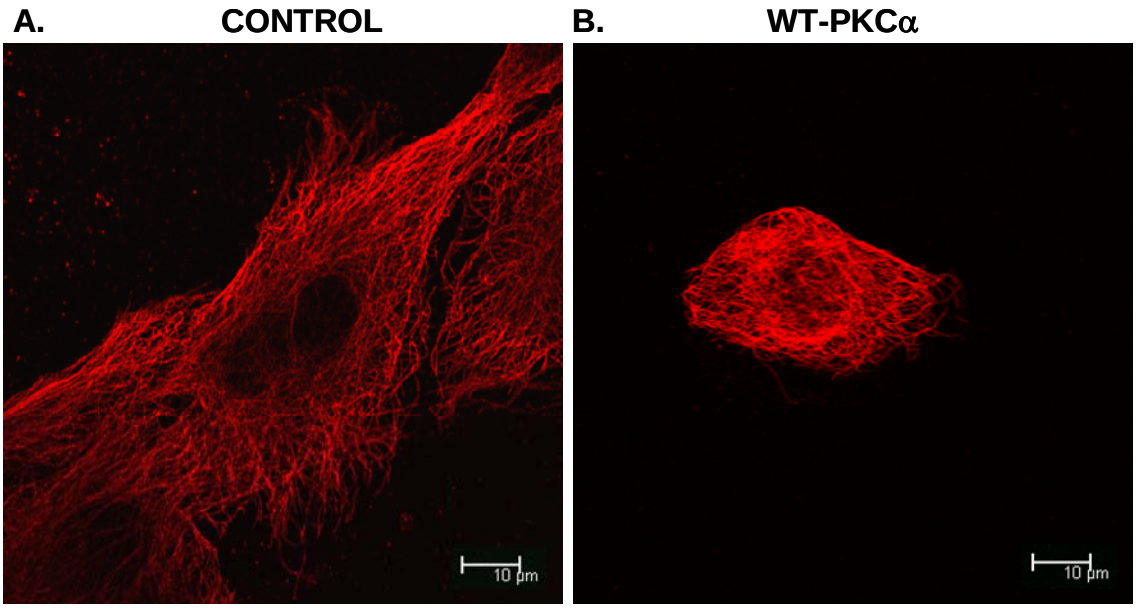

Figure 27. Effect of PKCα over-expression on microtubule structure in MCF-10A cells. Methanol-fixed cells were transfected with [A] the control vector (pCMV4), or [B] WT-PKCα. Visualization of endogenous α-tubulin present in microtubules was carried out with anti-α-tubulin monoclonal antibody (DM1A), followed by rhodamine-conjugated secondary antibody (Alexa fluor 594). The results were qualitatively identical in three independent experiments in which a minimum of 50 cells were inspected.

Effect on Microtubule Assembly by Tubulin Phosphorylation

To test whether phosphorylation of α6-tubulin at Ser-165 has any effect on microtubule formation, we tracked the incorporation of GFP signal into microtubules of cells expressing humanized *Renilla reniformis* GFP (hrGFP), hrGFP-S165D or hrGFP-S165N mutants, or hrGFP-WT-tubulin. After transfection, monomers were drained and the remaining cytoskeleton was fixed with ice-cold methanol to improve the visualization of

microtubules. Cells were double-stained with anti-hrGFP antibody and with anti-α-tubulin antibody. We observed a level of incorporation of hrGFP-WT-α6-tubulin or hrGFP-S165N-α6-tubulin (green) into microtubules that was comparable to the staining observed with the α-tubulin antibody (red). In contrast, when cells were transfected with the hrGFP-S165D mutant, far less hrGFP incorporation into microtubules was observed. Hence, a mutant that mimics phosphorylation of α6-tubulin, hrGFP-S165D is (Figure 28) only weakly incorporated into microtubules. Furthermore, the microtubule network of hrGFP-S165D resembles that produced in MCF-10A cells by over-expression of PKCα (Figure 27), while the pattern of incorporation of hrGFP-WT-α-tubulin or hrGFP-S165N-α6-tubulin resembles the microtubule structure of control cells (Figure 27). Taken together, these data support a model in which phosphorylation at Ser-165 by PKC(α) prevents incorporation of α6-tubulin monomers into microtubules, or causes disassembly of pre-existing microtubule polymers.

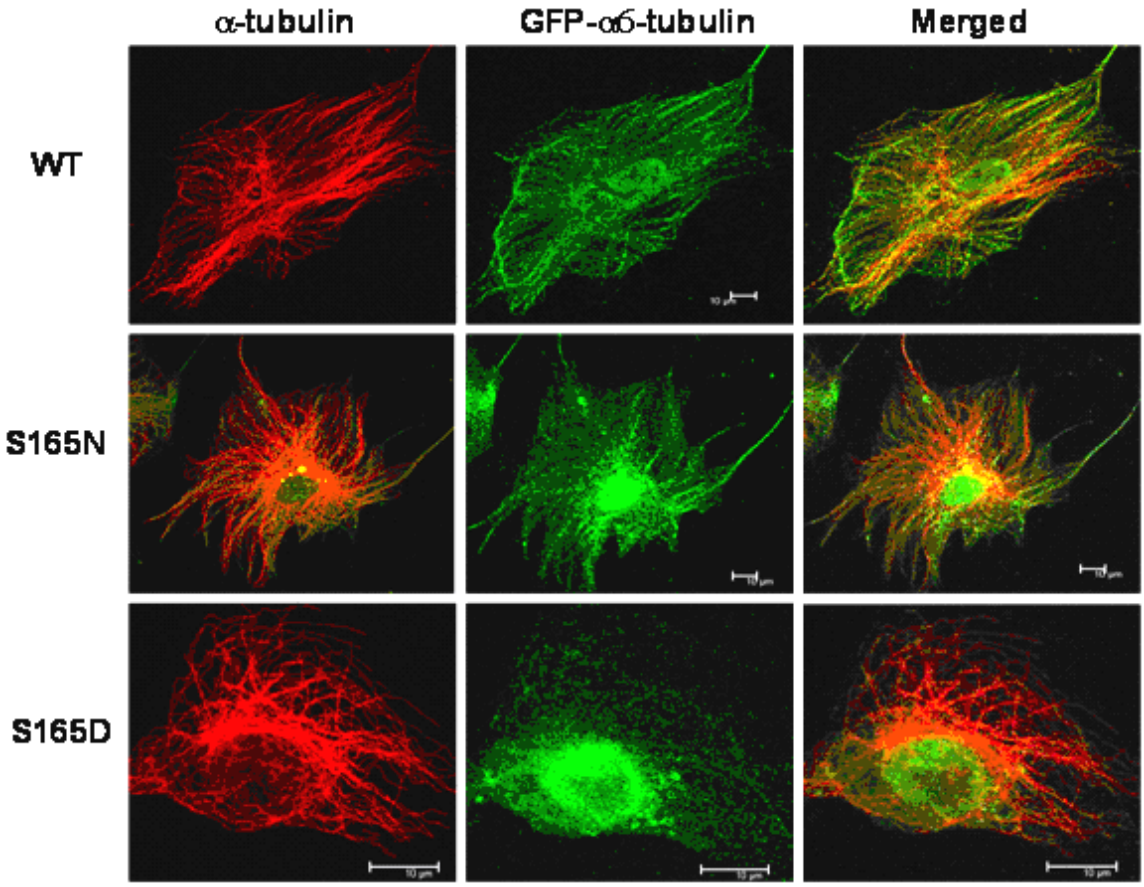

Figure 28. **Incorporation of GFP-α6-tubulin mutants into microtubules of MCF-10A transfectants.** Methanol-fixed cells were transfected with WT-GFP-α6-tubulin, or with either GFP-S165N or GFPS165D mutants of α6-tubulin. By use of confocal microscopy, incorporation of hrGFP-α6-tubulin was determined with a monoclonal hrGFP-antibody and a fluorescein-conjugated secondary antibody (Alexa fluor 488). Red fluorescent signals measured total α-tubulin incorporated into microtubules using anti-α-tubulin monoclonal antibody (DM1A) and rhodamine-conjugated secondary antibody (Alexa fluor 594). The results were qualitatively identical in three independent experiments in which a minimum of 50 cells were inspected for each construct.

Structural Significance of PKCα Phosphorylation to Tubulin Assembly

In an attempt to explain why phosphorylation of α-tubulin by PKCα may decrease polymerization, we looked at the position of Ser-165 in the three dimensional structure of two assembling α/β heterodimers.

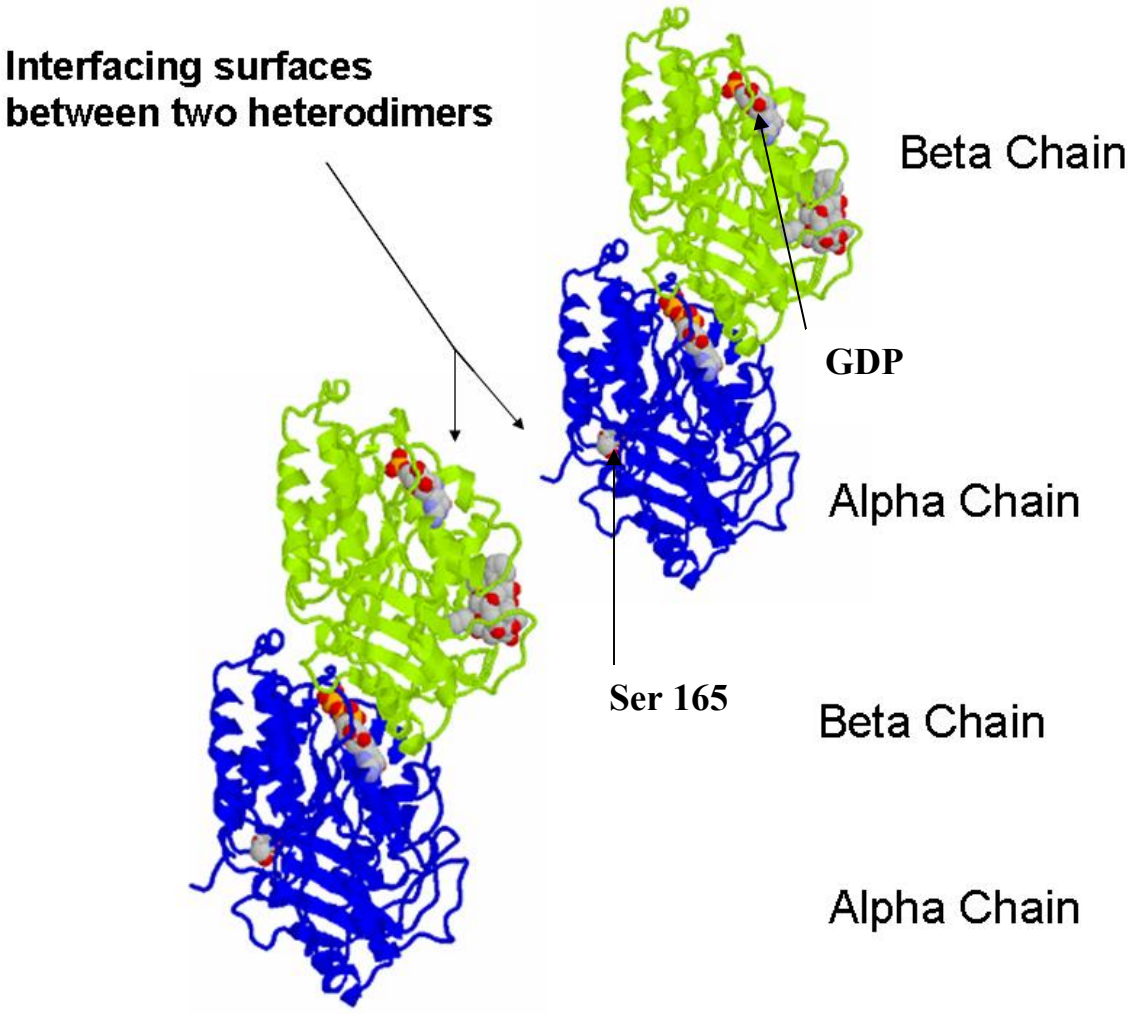

Figure 29. **Structural model of two interfacing heterodimers of tubulin.** The model identifies Ser-165 at the interface between two heterodimers of α/β−tubulin. Phosphorylation of α-tubulin at Ser-165 of the first heterodimer would create charge-charge repulsion with the phosphates of the exchangeable GDP/GTP on the β-subunit of the second heterodimer. This arrangement suggests that such repulsion would prevent the assembly of microtubules, or disrupt a pre-existing polymer. Molecular modeling of three-dimensional coordinates of the α/β-heterodimer (PDB entry 1TUB) was performed with Protein Explorer.

As shown in Figure 29, Ser-165 residue lies at the interface between two α/β-heterodimers. At this position, Ser-165 will come into close promimity to the exchangeable GDP/GTP nucleotide of the approaching β-tubulin. If Ser-165 is phosphorylated, the presence of a negatively charged phosphate group could induce charge repulsion in the nucleotide binding site that in turn could prevent polymerization, thereby leading to the truncated microtubule structure observed in Figure 28.

Discussion

In this study, we found that PKCα phosphorylates α6-tubulin both in vitro and in intact cells. Inspection of the α6-tubulin primary sequence indicates that it has four PKC consensus phosphorylation sites, among which Ser-165 and Thr-337 were strong candidates since both residues are flanked by at least two cationic residues. Individual mutation at each site to Asp to mimic phosphorylation, revealed that this modification of Ser-165, but not Thr-337, increased cell motility, a phenotype previously ascribed to PKCα in MCF-10A cells. This effect on motile behavior is likely to result from decreased α-tubulin incorporation into microtubules. Our findings imply that phosphorylation of α-tubulin (either in monomeric form or in intact microtubules) is central to the mechanism of cell movement.

Studies on fibroblasts have shown that cell migration is inhibited either by disruption of microtubule organization or by stabilization of microtubules[71,72]. The dynamic instability of microtubules, which consists of continuous polymerization/depolymerization events, is fundamental to cell migration. According to our structural model (Figure 27), Ser-165 is

located at the interface such that it can interfere with the exchangeable GTP bound to β-tubulin on an incoming heterodimer. We speculate that repulsion by a negatively-charged phosphate group at Ser-165 may accelerate the dynamic instability of the microtubule polymer. This phenomenon may explain the truncated microtubule network observed with the GFP-S165D mutant of α6-tubulin (Figure 26). To further support this argument, future studies will employ purified α and β tubulin monomers and highly pure, recombinant PKCα for analyzing an impact by phosphorylation on the rates of assembly or disassembly.

What is the molecular mechanism by which microtubule dynamics drives cell movement? Some evidence shows that Rac1 activation was abolished by Taxol[73]. This result indicates that activation of Rac1 requires microtubule instability. In order to drive cell migration, activation of Rac1 is known to promote actin polymerization and lamellipodial protrusion.

Previous studies from the Rotenberg laboratory indicated that endogenous Rac1 is a downstream participant in the motility pathway induced by PKCα over-expression in MCF-10A cells (Sun and Rotenberg, 1999). This idea was suggested by the partial inhibition of motility in cells stably expressing PKCα and transfected with dominant-negative Rac1. Thus, upon phosphorylation of α-tubulin by PKCα, microtubule dynamics accelerate thereby increasing Rac1 activation. Co-incident with these events is actin polymerization and the resulting lamellipodial protrusions that collaborate to drive cell migration.

Our findings on the roles of PKCα and α-tubulin in breast cell migration have important implications for controlling the metastasis of breast cancer cells. Thus, α-tubulin and PKCα may be potential therapeutic targets by which to inhibit metastasis during tumor cell invasion, and may add to the anti-cancer effect of Taxol. When wound healing is desired after vascular injury, agents that promote cell migration may have therapeutic value.

CONCLUDING STATEMENT

The results in this study demonstrated the design of a traceable mutant of PKCα that was used successfully to identify PKCα-specific substrates.

During the course of our work with the traceable kinase of PKCα, α6-tubulin was identified as a PKCα substrate. Our results support a model in which phosphorylation of α6-tubulin at Ser-165 by PKCα increases cell movement thereby reproducing a phenotype that was previously ascribed to PKCα. Using site-specific mutations at Ser-165, the importance of phosphorylation of α6-tubulin to its incorporation into microtubules was demonstrated. Our findings indicated that the pseudo-phosphorylated mutant was not extensively incorporated, unlike the wildtype and phosphorylation-resistant mutant. Thus, phosphorylation of α6-tubulin either prevents its incorporation into microtubules and/or disassembles pre-existing microtubules.

References

1. Toker, A. Signaling through protein kinase C; *Front. BioSci.* **3**, 1134-1147, 1998

2. Newton, A.C. Protein kinase C protocols; (Humana Press) 119-157, 2003

3. Musashi, M., Ota, S., and Shiroshita, N. The role of protein kinase C isoforms in cell proliferation and apoptosis; *Int. J. Hematol.***72**, 12-19, 2000

4. Ubersax, J.A., and Ferrell, J.E., Jr. Mechanisms of specificity in protein phosphorylation; *Nature Rev. Mol.Cell Bio.* **8**, 530-541, 2007

5. Newton, A. C. Regulation of the ABC kinases by phosphorylation: Protein kinase C as a paradigm.; *Biochem J.* **370**, 361-371, 2003

6. Newton, A.C. Regulation of protein kinase C; *Curr.Opin.Cell Bio.* **9**, 161-167, 1997

7. Liu, J-P. Protein kinase C and its substrates; *Mol.Cell Endocrinol.* **116**, 1-29, 1996

8 . Spitaler, M, and Cantrell, D.A. Protein kinase C and beyond; *Nature Immunol.* **8,** 785-790, 2004

9. Sonnenburg, E.D., Gao, T., and Newton, A. C. The phosphoinositide-dependent kinase, PDK-1, phosphorylates conventional protein kinase C isozymes by a mechanism that is independent of phosphoinositide 3-kinase; *J. Biol. Chem.* **276,** 45289-45297, 2001

10. Waldron, R. T., and Rozengurt, E. : Protein kinase C phosphorylates protein kinaseD activation loop Ser 744 and Ser 748 and releases autoinhibition by the pleckstrin homology domain; *J. Biol. Chem.* **278,** 154-163, 2003

11. Jaken, S., and Parker, P. J. : Protein kinase C binding partners; *BioEssays,* **22,** 245-254, 2000

12. O'Brian, C.A, Vogel, V. G., Singletary, S. E., and Ward, N. E. Elevated protein kinase C expression in human breast tumor biopsies relative to normal breast tissue; *Cancer Res.* **49,** 3215-3217, 1989

13. Ways, D.K., Kukoly, C.A., deVente, J., Hooker, J.L., Bryant, W.O., Posekany, K.J., *et al.* MCF-7 breast cancer cells transfected with protein kinase C-α exhibit altered expression of other protein kinase C isoforms and display a more aggressive phenotype; *J. Clin. Invest.* **95,** 1906-1915, 1995

14. Soule, H. D., Maloney, T. M., Wolman, S. R., Peterson, W. D., Jr., Brenz, R., McGrath, C. M., Russo, J., Pauley, R. J., Jones, R. F., and Brooks, S. C. Isolation and

characterization of a spontaneously immortalized human breast epithelial cell line, MCF-10A; *Cancer Res.* **50,** 6075-6086, 1990

15. Sun, X.-g., and Rotenberg, S.A., Overexpression of protein kinase Cα in MCF-10A human breast cells engenders dramatic alterations in morphology, proliferation, and motility; *Cell Growth Diff.* **10,** 343-352, 1999

16. Liu, B., Rotenberg, S.A., Mirkin, M.V. Scanning electrochemical microscopy of living cells: Imaging redox reactivities; *Proc. Natl. Acad. Sci*. **97,** 9855-9860, 2000

17 Woodhouse, E. C., Chuaqui, R. F., and Liotta, L. A. General mechanisms of metastasis; *Cancer Res.* **80***,* 1529–1537, 1997

18. Ananthakrishnan, R., and Ehrlicher, A.: The forces behind cell movement; *Int. J. Biol. Sci,.* **3(5),** 303–317, 2007

19. Wittmann, T. and Waterman-Storer, M.,: Cell motility: can Rho GTPases and microtubules point the way; *J. Cell Sci.***114**, 3795-3803, 2001

20. Nogales, E., Wolf, S.G., and Downing, K.H., Structure of the αβ tubulin dimer by electron crystallography; *Nature,* **391,** 199-203, 1998

21. Ludvena, R.F., The multiple forms of tubulin: different gene products and covalent modifications; *Int. Rev. Cyt.* **178,** 207-275, 1998

22. Idriss, H.T. Three steps to cancer: How phosphorylation of tubuli, tubulin tyrosine ligase and P-glycoprotein may generate and sustain cancer; *Cancer Chem. Pharm.,* **54,** 101-104, 2004

23. Vuori, K. and Ruoslahti, E. Activation of protein kinase C precedes 5β1 integrin-mediated cell spreading on fibronectin; *J. Biol. Chem.* **268**, 21459-21462, 1993

24. Schliwa, M., Nakamura, T., Porter, K.R., and Euteneuer, U, A tumor promoter induces rapid and coordinated reorganization of actin and vinculin in cultured cells; *J. Cell Biol.* **99,** 1045 -1059, 1984

25. Goodnight, J., Mischak, H., Kolch, W., and Mushinski, J. F. Immunocytochemical localization of eight protein kinase C isozymes overexpressed in NIH 3T3 fibroblasts. Isoform-specific association with microfilaments, Golgi, endoplasmic reticulum, and nuclear and cell membranes*; J. Biol. Chem.*, **270,** 9991–10001, 1995

26. Jirousek , M.R., Goekjian, P.G.: Protein kinase C inhibitors as novel anticancer drugs; *Expert Opinion on Investig. Drugs*, **10,** 2117-2140, 2001

27. Manning, G., Whyte, D.B., Martinez, R., Hunter, T., and Sudarsanam, S.: The protein kinase complement of the human genome; *Science* **298**, 1912–1934, 2002

28. Tyers, M.,Haslam, R. J., Rachubinski, R. A, and Harley, C. B., Molecular analysis of pleckstrin: the major protein kinase C substrate of platelets; *J. Cell Biochem.* **40,** 133-145, 1989

29. Poole, W.P., Pula, G., Hers, I., Crosby, D., and Jones, M. L., PKC-interacting proteins: from function to pharmacology; *Trends Pharmacol. Sci.***25,** 528-535, 2004

30. Buzko, O., and Shokat., K.M. : A kinase sequence database: sequence alignments and family assignment; *Bioinform.* **18(9)**, 1274-1275, 2002

31. Fukunaga, R., and Hunter, T.: MNK1 a new MAP kinase-activated protein kinase, isolated by a novel expression screen for identifying protein kinase substrates; *EMBO J.* **16**, 1921–1933, 1997

32. Eblen, S. T., Kumar, N. V., Shah, K., Henderson, M. J., Watts, C. K. W., Shokat, K.M., and Weber, M. J., Identification of novel ERK2 substrates through use of an engineered kinase and ATP analogs; *J. Biol. Chem.* **287,** 14926-14935, 2003

33. Shah K., Liu Y., Deirmengian, and Shokat K.M. Engineering unnatural nucleotide specificity for Rous sarcoma virus tyrosine kinase to uniquely label its direct substrate; *Proc. Natl. Acad. Sci. USA* **94,** 3565-3570, 1997

34. Liu, Y., Shah, K., Yang, F., Witucki, L., and Shokat, K.M. Engineering src family protein kinases with unnatural nucleotide specificity; *Chem. Biol*. **5**, 91-101, 1998

35. Liu, Y., Shah, K., Yang, F., Witucki, L., and Shokat, K.M. A molecular gate which controls unnatural ATP analogue recognition by the tyrosine kinase v-src; *Bioorg. Med. Chem*. **6**, 1219-1226, 1998

36. Liu, Y., Bishop, A., Witucki, L., Kraybill, B., Shimizu, E., Tsien, J., Ubersax, J., Blethrow, J., Morgan, D.O., and Shokat, K.M. Structural basis for selective inhibition of src family kinases by PPI; *Chem. Biol*, **6**, 671-678, 1999

37. Habelhah, H., Shah, K., Huang, L., Burlingame, A. L., Shokat K.M., and Ronai, Z. Identification of new JNK substrate using ATP pocket mutant JNK and a corresponding ATP analogue; *J. Biol. Chem.* **276**, 18090-18095, 2001

38. Witucki, L.A, Huang, X., Shah, K., Liu, Y., Kyin, S., Eck, M., and Shokat, K.M. Mutant tyrosine kinases with unnatural nucleotide specificity retain the structure and phosphor-acceptor specificity of the wild-type enzyme; *Chem. Biol*. **9**, 25-33, 2002

39. Xu, Z.-b., Chaudhary, D., Olland, S., Wolfrom, S., Czerwinski, R., Malakian, K., *et al*.; Catalytic domain crystal structure of protein kinase Cθ; *J. Biol. Chem.* **279,** 50401-50409, 2004

40. Krishnan, K.S., Rikny, R., Rao, S., Shiverlkumar, M., Mosko, M., Narayanan, R., Etter, P., Estes, P.S., Ramaswami, M.; Nucleoside diphosphate kinase, a source of GTP, is required for dynamin-dependent synaptic vesicle recycling; *Neuron.* **30,** 197-210, 2001

41. Glass, D. B., and Krebs, E. G., Comparison of the substrate specificity of adenosine 3':5'-monophosphate and guanosine 3':5'- monophosphate dependent protein kinases; *J. Biol. Chem.* **254,** 9728-9738, 1979

42. Batchelor, M., and Schenk, J.O., Protein kinase A activity may kinetically upregulate the striatal trasporter for dopamine; *J. Neuroscience.* **18,** 10304-10309, 1998

43. Ward, N.E., and O'Brian, C.A., Kinetic evidence of protein kinase C by staurosporine: Evidence that inhibition entails inhibitor binding at conserved region of the catalytic domain but not competition with substrates; *Mol. Pharmacol.* **41,** 387-392, 1991

44. Garcia, B.A., Hake, S.B., Diaz, R.L., Kauer, M., Morris, S.A., Recht, J., Shababowitz, J., Mishra, N., Strahl, B.D.,Allis, C.D., and Hunt, D.F. Organismal differences in post-translational modifications in histones H3 and H4; *J. Biol. Chem.* **282,** 7641-7655, 2007

45. Ransom, W.D., Lao, P.-C., Gage, D.A., and Boss, W.F. Phosphoglyceryl-ethanolamine posttranslational modification of plant eukaryotic elongation factor 1α; *Plant Physiol.*, **117,** 949–960, 1998

46. Takeuchi, F., Hashimoto, E., and Yamamura, H., Phosphorylation of histone H2A by protein kinase C and identification of the phosphorylation site; *J. Biochem.* **111,**788-792, 1992

47. Huang, W., Mishra, V., Batra S., Dillon I., and Mehta, K.D.; Phorbol ester promotes histone H3-Ser10 phosphorylation at the LDL receptor promoter in a protein kinase C-dependent manner; *J. Lipid Res.,* **45,** 1519-1527, 2004

48. Peters, H. I., Chang, Y. W., and Traugh, J. L., Phosphorylation of elongation factor 1 (EF-1) by protein kinase C stimulates GDP/GTP-exchange activity; *Eur. J. Biochem.* **234,** 550-556, 1995

49. Eggert, M., Radomski, N., Tripier, D., Traub, P., and Jost, E., Identification of phosphorylation sites on murine nuclear lamin C by RP-HPLC and microsequencing; *FEBS Lett,* **292,** 205-209, 2002

50. Li, G. C., He, F., Shao, X., Urano, M., Shen, L., Kim, D., Borrelli, M., Leibel, S. A., Gutin, P. H. and Ling, C. C.: Adenovirus-mediated heat-activated antisense Ku70 expression radiosensitizes tumor cells *in vitro* and *in vivo; Cancer Res.,* **63,** 3268-3274, 2003

51. Muller, C., Paupert, G., Monferran,, S., Salles, B.: The double life of Ku protein: Facing the DNA breaks and the extra cellular environment; *Cell Cycle,* **4**, 438-441, 2005

52. Obermann, W.M., Sondermann, H., Russo, A.A., Pavletich, N.P., and Hartl, F.U.: In vivo function of Hsp90 is dependent on ATP binding and ATP hydrolysis; *J. Cell Biol.,* **143,** 901-910, 1998

53. Bagatell, R., and Whitesell, L.: Altered Hsp90 function in cancer: A unique therapeutic opportunity; *Molecular Cancer Therapeutics,* **3,** 1021-1030, 2004

54. Verdier-Pinard, P., Wang, F., Burd, B., Angeletti, R. H., Horwitz, S. B., and Orr, G. A.: Direct analysis of tubulin expression in cancer cell lines by electrospray ionization mass spectrometry; *Biochemistry* **42,** 12019-12027, 2003

55. Habelhah H., Shah, K., Huang, L., Burlingame, A. L., Shokat K. M., and Ronai, Z; *J. Biol. Chem.* **276,** 18090-18095, 2001

56. Penque, D., Galego, L., and Rodrigues-Pousada, C.: Mulitiple α-tubulin isoforms in cilia and cytoskeleton of Tetrahymena pyriformis generated by post-translational modifications; *Eur. J. Biochem.,* **195,** 487-494, 1991

57. Westermann, S., and Weber, K.: Post-translational modifications regulate microtubule function; *Nat. Rev. Mol. Cell. Biol.* **4,** 938–947 2003

58. Wittmann, T., and Waterman-Storer, C. M. : Cell motility: can Rho GTPases and microtubules point the way?; *J. Cell Sci.*, **114,** 3795-3803, 2001

59**.** Correas, I., Diaz-Nido, J., and Avila, J., Microtubule-associated protein tau is phosphorylated by protein kinase C on its tubulin binding domain; *J. Biol. Chem*., **267,** 15721-15728, 1992

60. Robinson, P.J., The role of protein kinase C and its neuronal substrates; *Mol. Neuro. Biol.,* **5,** 87-130, 1991

61. Kiley, S.C., and Parker, P.J., Differential localization of protein kinase C isozymes in U937 cells: evidence for distinct isozyme functions during monocyte differentiation; *J Cell. Sci.* **108,** 1003-1016, 1995

62. Kiley, S.C., and Parker, P.J., Defective microtubule reorganization in phorbol ester-resistant U937 variants: reconstitution of the normal cell phenotype with nocodazole treatment; *Cell Growth Diff.* **8,** 231-242, 1997

63. Takahashi, M., Mukai, H., Oishi, K., Isagawa, T., and Ono Y. Association of immature hypophosphorylated protein kinase Cε with an anchoring protein CG-NAP; *J. Biol. Chem.* **275,** 34592-34596, 2000

64. Volkov, Y., Long, A., and Kelleher, D., Inside the crawling T cell: Leukocyte function-associated antigen-1 cross-linking is associated with microtubule-directed translocation of protein kinase C isoenzymes ß(I) and δ; *J. Immunol.* **161,** 6487-6495, 1998

65. Volkov, Y., Long, A., McGrath, S., Ni Eidhin., and Kelleher, D., Crucial importance of PKC-beta (I) in LFA-1-mediated locomotion of activated T cells; *Nat. Immunol.* **2,** 508-514, 2001

66. Yoshida, N., Haga, K., and Haga, T., Identification of sites of phosphorylation by G-protein –coupled receptor kinase 2 in β-tubulin; *Eur. J. Biochem.***270,** 1154-1163, 2003.

67. Casas, B., Calabokis, M., Kurz, L., Galan-Caridad, J.M., Bubis, J., and Gonzatti, M. I., Trypanosoma *cruzi:*in vitro phosphorylation of tubulin by a protein kinase CK2-like enzyme; *Exp. Parasitol.* **101,** 129-137, 2002

68. Khan, I. A., and Luduena, R.F., Phosphorylation of β_{iii}-Tubulin; *J. Biochem.* **35,** 3704-3711, 1996

69. Stapulionis, R, and Deutscher, M. P., Permeabilized mammalian cells as a system for protein synthesis, *Meth. Mol. Biol* ,**77**, 23-30, 2001

70. House, C., Wettenhall, R. E., and Kemp, B. E., The influence of basic residues on the substrate specificity of protein kinase C. *J. Biol. Chem,* **262,** 772-777, 1987

71. Liao, G., Nagasaki, T., and Gundersen, G.G.: Low concentrations of nocodazole interfere with fibroblast locomotion without significantly affecting microtubule level: Implications for the role of dynamic microtubules in cell locomotion. *J.Cell Sci*., **108**, 3473–3483, 1995

72. Mikhailov, A., and Gundersen, G.G.: Relationship between microtubule dynamics and lamellipodium formation revealed by direct imaging of microtubules in cells treated with nocodazole or taxol;.*Cell Motil Cytoskel.*, **41**, 325–340, 1998

73. Hu, Y.-L., Li, S., Miao, H., Tsou, T.C., Angel del Pozo, M., and Chien, S. Roles of microtubule dynamics and small GTPase Rac in endothelial cell migration and lamel-lipodium formation under flow; *J. Vasc.* **39,** 465–476, 2002